ABSTRACT

Title of Document:	PACKAGING OF AN IRON-GALLIUM NANOWIRE ACOUSTIC SENSOR
	Ronald J. DiSabatino Jr., M.S., 2006
Directed By:	Associate Professor F. Patrick McCluskey, Department of Mechanical Engineering

The development of packaging for an underwater acoustic sensor is a more complex task than package design for a typical microelectronic device because of the need to simultaneously protect the device from the environment while allowing interaction with it. A bio-inspired package, based on the hearing mechanisms in aquatic animals, has been developed for this purpose. The package will ensure reliability in the underwater environment while not interfering with the transmission of sound. The package is designed to contain a nanowire sensor in a fluid medium, leaving the wires free to move. Materials matching the acoustic impedance of seawater are incorporated to allow sound to penetrate the package. Acoustic properties of various materials were investigated using scanning acoustic microscopy for this application. A prototype package was fabricated, and tests were performed to evaluate the impedance match between the selected materials and seawater.

PACKAGING OF AN IRON-GALLIUM NANOWIRE ACOUSTIC SENSOR

By

Ronald J. DiSabatino Jr.

Thesis submitted to the Faculty of the Graduate School of the
University of Maryland, College Park, in partial fulfillment
of the requirements for the degree of
Masters of Science in
Mechanical Engineering
2006

Advisory Committee:
Associate Professor F. Patrick McCluskey, Chair
Professor Alison B. Flatau
Associate Professor Peter Sandborn

Dedication

To my grandparents:

Remo and Helen DiSabatino, and Bartolo and Columba Todarello

Acknowledgements

First and foremost, I thank my parents, Ron and Joanne, and my sister, Laura. Their unending support and encouragement have put me where I am today. Throughout my college career I have relied on the advice and support of many. I thank my advisor, Dr. Patrick McCluskey, for giving me the opportunity to work on this project and for his direction. I also appreciate the help and guidance I have received from Dr. Alison Flatau. Thank you to Jan Lindberg for supporting this work, as well as Marilyn Wun-Fogle and Jim Restorff at NSWC. My accomplishments would not be possible with out insight from my fellow students: Karumbu Meyyappan, Kaushik Ghosh, Anshul Shrivastava, Yunqi Zheng, Rui Wu, Zhixiang Wang, Tim Seeley, Lauren Everhart, Adam McClure, Rupal Jain, Pedro Quintero, Pat Downey, Dr. Jin Yoo, Supratik Datta, Jayasimha Atulasimha, Luke Twarek, Kate Hale and Chaitanya Mudivarthi. I also thank Dr. Beth Stadler and Patrick McGary at the University of Minnesota for their collaboration. I appreciate all the help from Jon Hummel and Tom Loughran in the cleanroom, Howard Grosenbacher in the machine shop, and thank Dr. Smela for introducing me to MEMS. I am grateful to Bryan Charboneau, Eric Shields, Kevin Genson, and Austin Cox for their friendship and support. And finally, thank you Heather for being with me every step of the way.

This work was supported by Office of Naval Research Grant # N000140310954, Program Officer Jan F. Lindberg, ONR 321, Sensors, Sources, & Arrays.

Table of Contents

Chapter 1: Introduction

1.1 Galfenol nanowire acoustic sensors

Galfenol ($Fe_{1-x}Ga_x$) is increasingly being studied as a material for acoustic sensing because of its unique combination of magnetostriction [1] and advantageous mechanical properties. These properties include its strong tensile strength (~500 MPa) [2] and high ductility, which are important in bending applications [3], and permit Galfenol to be used in the creation of nanowire acoustic sensors where arrays of cantilevered nanowires interact with incoming sound waves [4] Figure 1 shows such an array of nickel nanowires fabricated at the University of Minnesota. Acoustic pressure induced bending of the Galfenol nanowires creates changes in magnetic fields that can be picked up by a giant magnetoresistance (GMR) sensor attached to the base of the nanowires, thereby turning sound into an electrical signal. Figure 2 shows an example of a GMR sensor from NVE Inc., Eden Prairie, Minnesota. By having nanowires with different lengths and diameters positioned over one GMR sensor, a sensor can pick up a wide range of frequencies, much like the human ear.

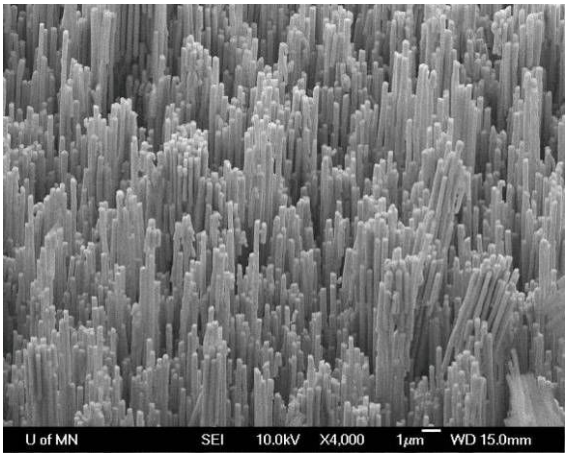

Figure 1. SEM image of a nanowire array [4].

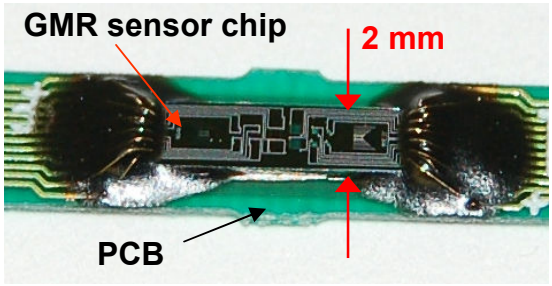

Figure 2. A GMR sensor from NVE, Inc.

Research is ongoing to characterize Galfenol's behavior in bending applications. Downey et al. [3] have shown that sinusoidal forces on a cantilevered beam with an applied bias magnetic field resulted in measurable periodic induction in the beam. The work was done on Galfenol beams with a 3.18 mm diameter and lengths ranging from 24.82 mm to 57.28 mm. The rods were clamped at one end and excited by a dynamic shaker attached to the other end. Measurements were taken using both a pickup coil wrapped around the rod as well as a GMR sensor located at the clamped end of the rod. Though the rods tested are much larger than the nanowires, the work done showed that, on the macroscopic scale, the bending of a Galfenol rod can be sensed by both a GMR sensor and a pickup coil. The parts of the beam that are in tension and compression do not result in zero net induction. This is promising if the concept of sensing bending Galfenol beams is to be scaled down to the nano-scale.

Past work in the study of nanowire characterization and manipulation has shown it is possible to manipulate and image nanowires at resonant frequencies. Dikin et al. have shown that nanowires can be excited at their resonant frequencies [5]. The work focused on using the mechanical resonance of cantilevered SiO_2 nanowires to find their bending modulus. Nanowires were attached to a bimorph piezodriver inside an SEM. The nanowires were successfully excited electrically with an AC electrical field

and mechanically with the piezodriver. The SEM captured images of the wires in different resonant modes, and the frequencies were used to calculate the bending modulus of the nanowires which was found to be about 47 GPa instead of 72 GPa which is the accepted value for bulk fused silica fibers.

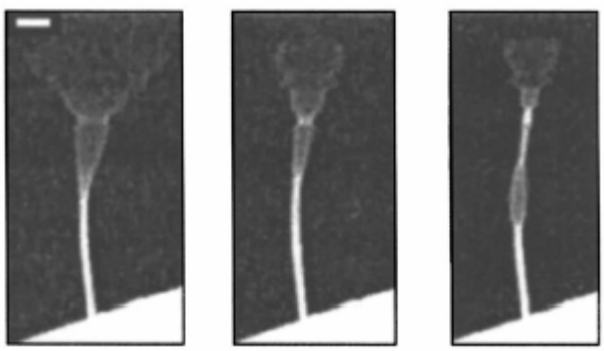

Figure 3. An image of a resonating SiO2 nanowire from [5].

Yu et al. have designed an implemented a nanomanipulator system that fits inside an SEM [6,7]. Much like the work of Dikin et al, the nanomanipulator setup was used to excite nanowires at resonant frequencies [6]. The setup has also been used for examining carbon nanotubes [7]. Under the inspection of an SEM, the nanotubes were picked up and fixed to AFM cantilevers where they could be manipulated and bent while measuring properties such as stiffness and conductivity.

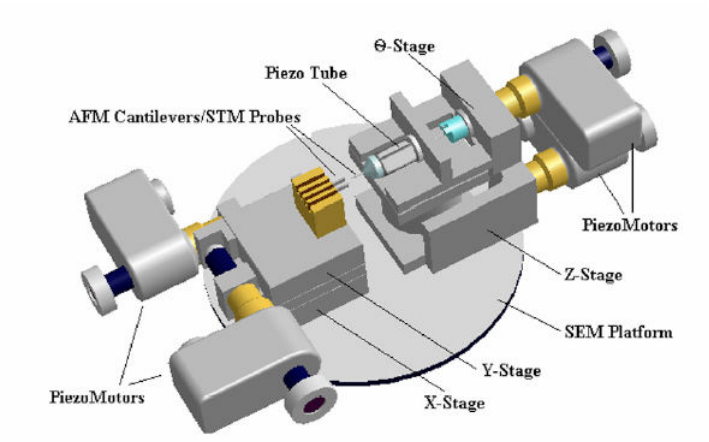

Figure 4. A drawing of Yu et al.'s nanomanipulator setup from [7].

A similar approach is taken by Downey et al. for studying Galfenol nanowires for their use in acoustic sensing applications [8]. A custom manipulator setup is currently being designed and fabricated that will allow the study of single nanowires. Not only is it necessary to be able to bend and excite the nanowires, but the magnetostrictive properties must also be characterized on this scale if they are to be deployed in an acoustic sensor application.

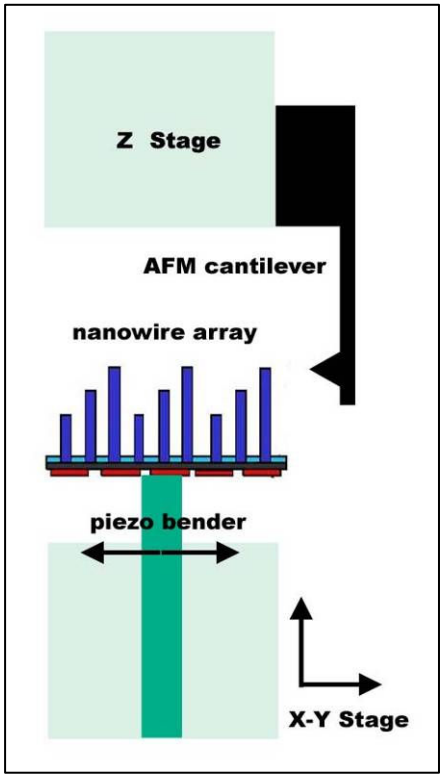

Figure 5. A drawing of the proposed nanowire manipulation setup.

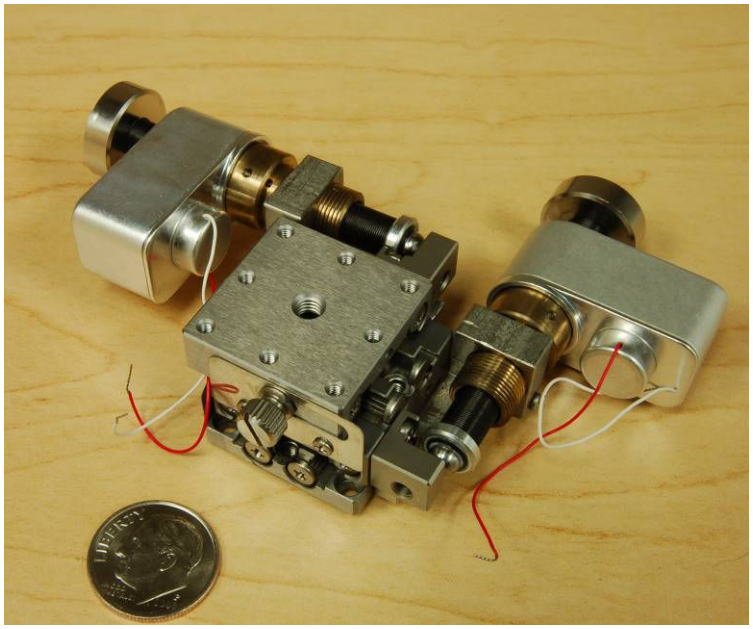

Figure 6. The x-y stage and piezodriven motors.

The manipulator setup (Figure 5) shows a nanowire array fixed to a piezobender mounted on a high resolution (30 nm) stage (Figure 6). A second stage with an AFM probe attached to it is used to manipulate individual or groups of nanowires. Integration of GMR sensors into this setup will allow measurements of changes in magnetic induction to be done during different experiments such as excitation of the arrays at different frequencies, static bending and quasi-static bending of the nanowires. These tests will further develop magnetostrictive nanowires for sensor applications.

1.2 Nanowire Fabrication

Galfenol nanowires, with diameters from 20 to 200 nm and lengths around 10 to 15 μm, are created by electrochemically depositing the alloy into the pores of an alumina template [4]. The process begins by anodizing a layer of aluminum, creating a porous template into which nanowires can be grown. Commercial templates are available

that have unordered pores of non-uniform diameter. McGary et al. [4] have shown that by imprinting the aluminum surface with a nitride stamp and controlling anodization conditions, it is possible to create ordered pores with uniform diameters and spacing. Furthermore, the pores extend collinearly through the alumina creating straight through holes that are ideal for growing nanowire arrays. Figure 7 shows an AFM image of the aluminum surface after being stamped. Figure 8 is taken after anodization and at a magnification where the stamped and unstamped regions are visible.

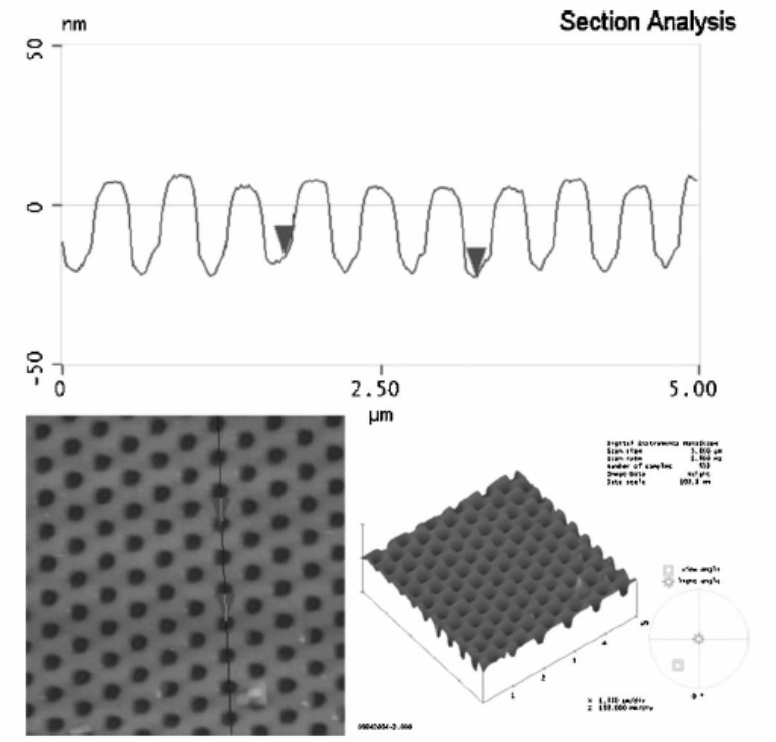

Figure 7. An AFM image of an electropolished aluminum surface after being imprinted with a nitride stamp [4].

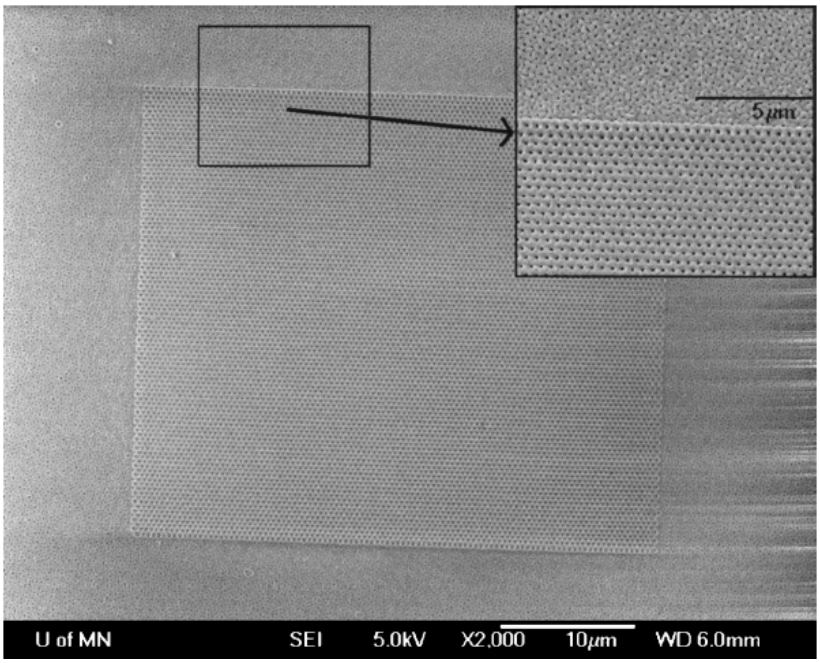

Figure 8. An SEM of the anodized alumina template. Notice the ordering in the area that was stamped compared to unstamped region [4].

After the porous alumina layer is grown, the seed layer is etched off the back as well as the base of the alumina layer leaving through holes in the template. A copper electrode is deposited on the back of the template and the metal can then be electrochemically deposited into the pores. After the Galfenol deposition, the alumina template is etched back revealing the nanowires.

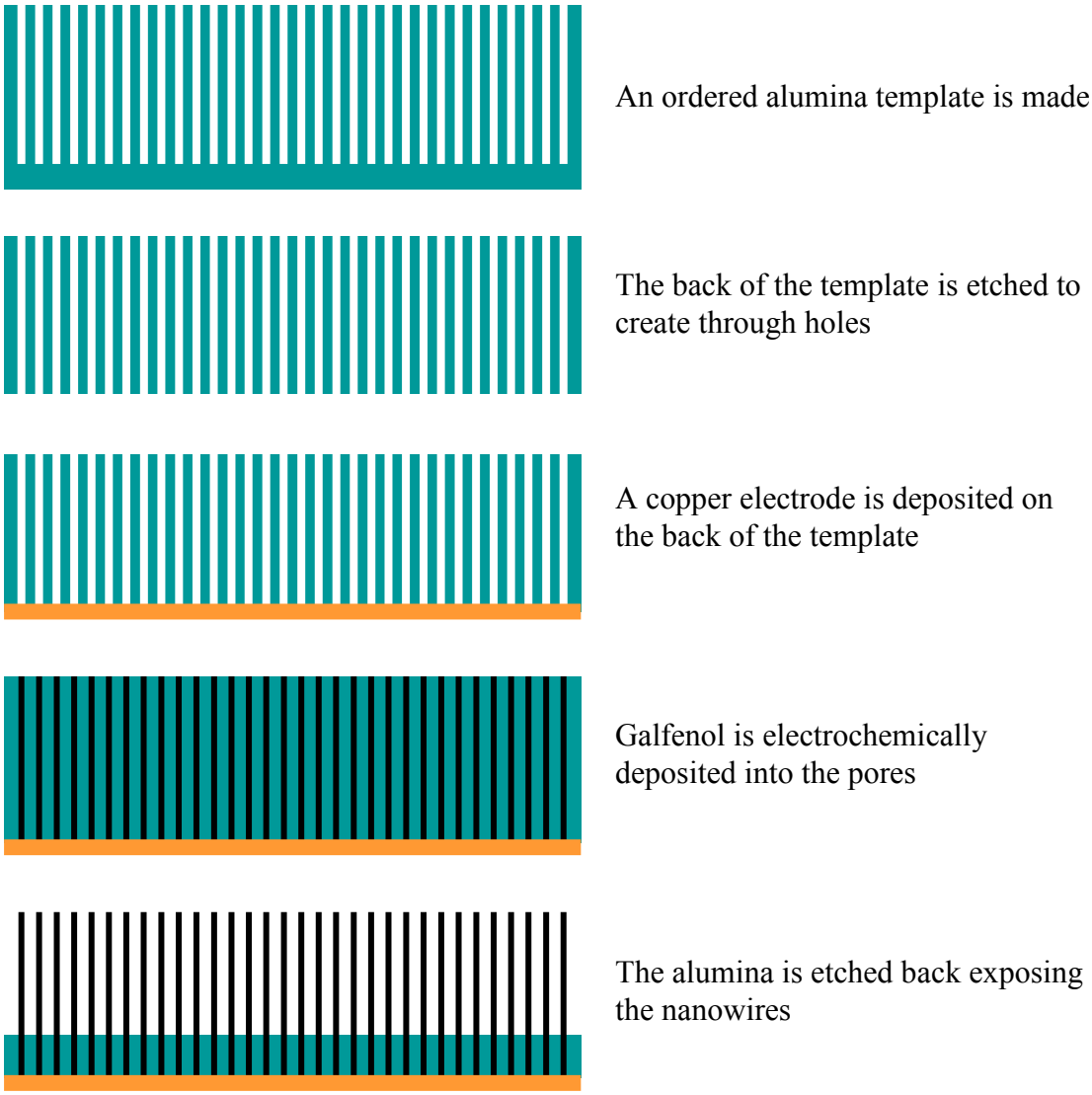

Figure 9. The nanowire fabrication process.

1.3 Acoustic Sensors

The following are examples of different types of micromachined underwater acoustic sensors and one example of a bio-inspired design for an acoustic sensor modeled after the human cochlea. The examples represent different approaches to microfabricating underwater transducers, and packaging for these types of devices is discussed in the next chapter.

Bernstein et al. (1997) fabricated and tested a ferroelectric sonar transducer utilizing PZT ($PbZrTiO_3$) to sense the vibration of a silicon membrane [9]. The device (Figure 10) operates in the ultrasonic range from 0.3 to 2 MHz. A layer of PZT is deposited onto the top side of the wafer using a sol-gel process. The membrane is formed by an anisotropic wet etch with EDP. A p+ doped region stops the etch, leaving a 10 µm thick membrane. Dimensions of the devices range from 0.2 mm to 1 mm and the authors reported sensitivities reaching -235 dB re 1 V / µPa.

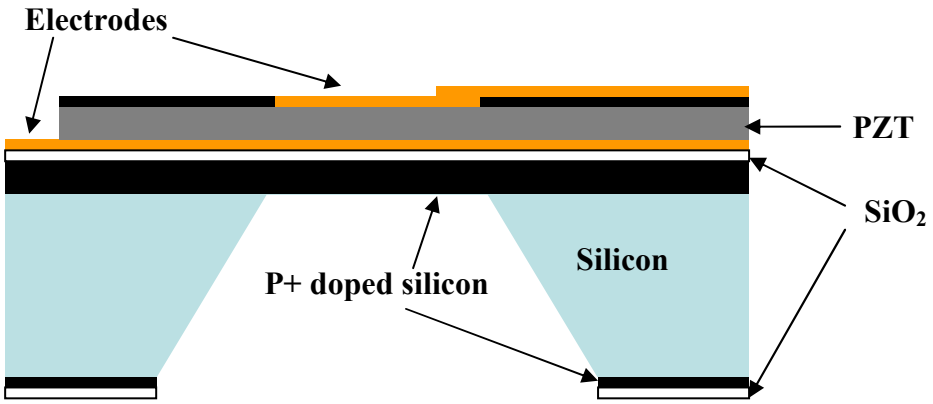

Figure 10. Figure adapted from [9] illustrating the PZT transducer.

Another design by Bernstein (1992) is a condenser hydrophone, where two electrodes, one of which is fixed, create a capacitor [10]. The movement of the second electrode due to acoustic vibrations creates changes in the capacitance. The moving electrode is formed in a similar way to the previous device with an EDP etch and a p+ etch stop defining the membrane. The size of the devices was approximately 1 mm and had a reported sensitivity of -206 dB re 1 V / µPa. It was tested from 200 Hz to 2 kHz.

Alkoy et al. fabricated and tested transducers made from hollow ceramic spheres [11]. The spheres were fabricated by creating bubbles out of a slurry of PZT, a polymer, and acetone. The bubbles were then sintered and had electrodes deposited on the inside and outside walls. Spheres with diameters from 1mm to 6mm and wall thicknesses from 12 µm to 150 µm were made. The devices achieved a sensitivity of -215 dB re 1 V / µPa, and were tested for frequencies from 5 kHz to 90 kHz.

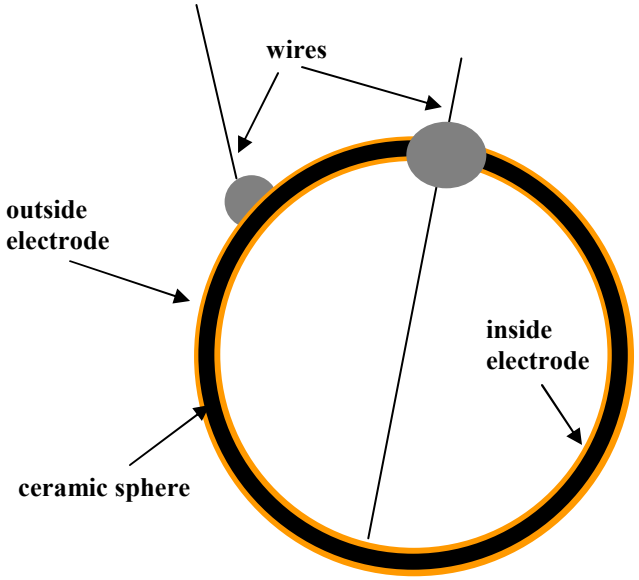

Figure 11. Figure adapted from [11] illustrating the hollow sphere transducers.

Mescher et al. fabricated a 3-D PZT shell on a silicon substrate creating a device designed to operate at 1-5 MHz [12]. The shell was made using a sacrificial carbon structure over which electrodes and PZT were deposited. Final devices used eight of these shell structures in parallel. Individual shells were 350 x 60 µm and had a height of 3.8 µm. Sensitivity of the devices was reported between -230 and -245 dB re 1 V / µPa.

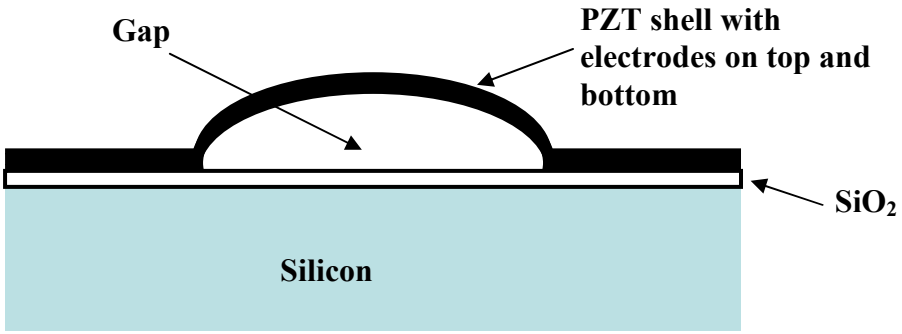

Figure 12. Figure adapted from [12] illustrating the PZT microshell on a silicon substrate.

Zhu et al. used a film of polyvinylidene diflouride (PVFD), a piezoelectric polymer, along with a MOSFET fabricated onto a silicon substrate [13]. Sound waves impacting the PDVF create a potential that controls the gate of the MOSFET. The device achieved sensitivities of -211.2 dB re 1 V/ μPa.

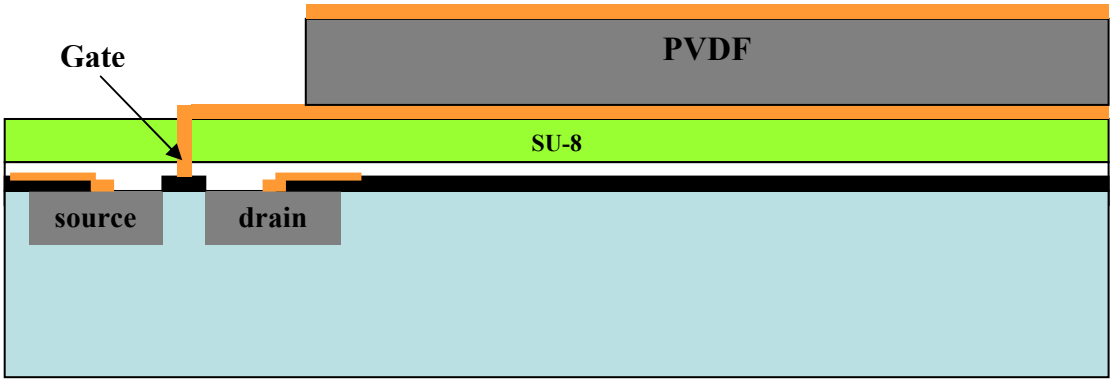

Figure 13.. Figure adapted from [13]. The PVDF-MOSFET device

R. D. White and K. Grosh have designed and microfabricated a model of the human cochlea [15]. Located in the inner ear, the cochlea senses different frequencies at different locations along its length (Figure 14). The microfabricated version uses a tapered membrane to achieve similar results.

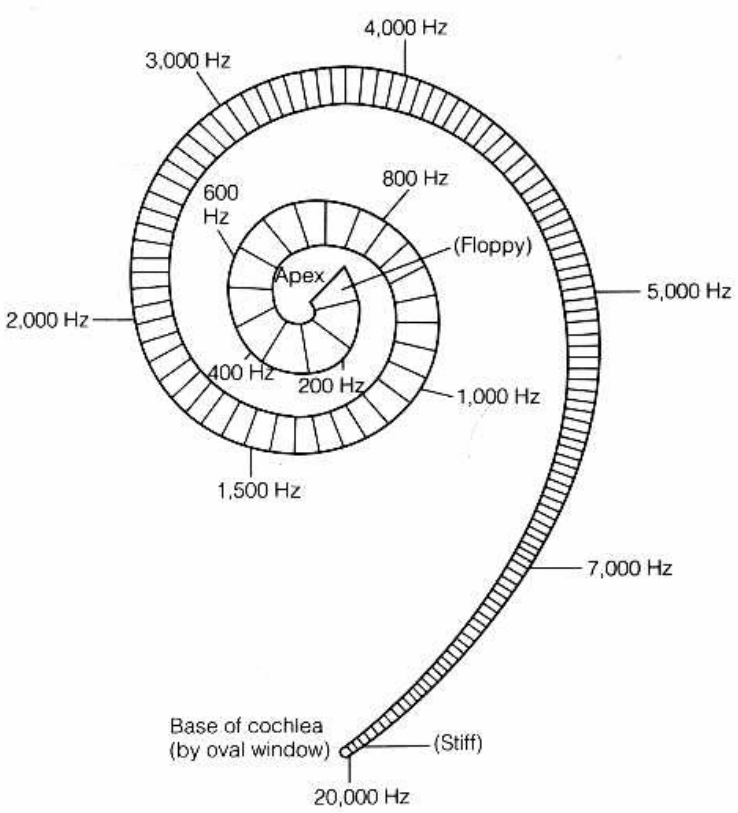

Figure 14. A drawing of the cochlea with the locations of sensitivity to different freqencies labeled from [15].

The membrane encloses a fluid filled duct. Sound enters the duct through an input membrane and travels down the length of the tapered membrane. Membrane movement is sensed with 32 capacitors spaced along its length. Because the membrane is tapered, different areas along the length are sensitive to different frequencies of sound. Like the cochlea, the narrow and wide end sense high and low frequency, respectively. As a result, each capacitor along the length senses a different frequency of sound from 100 Hz to 10 kHz.

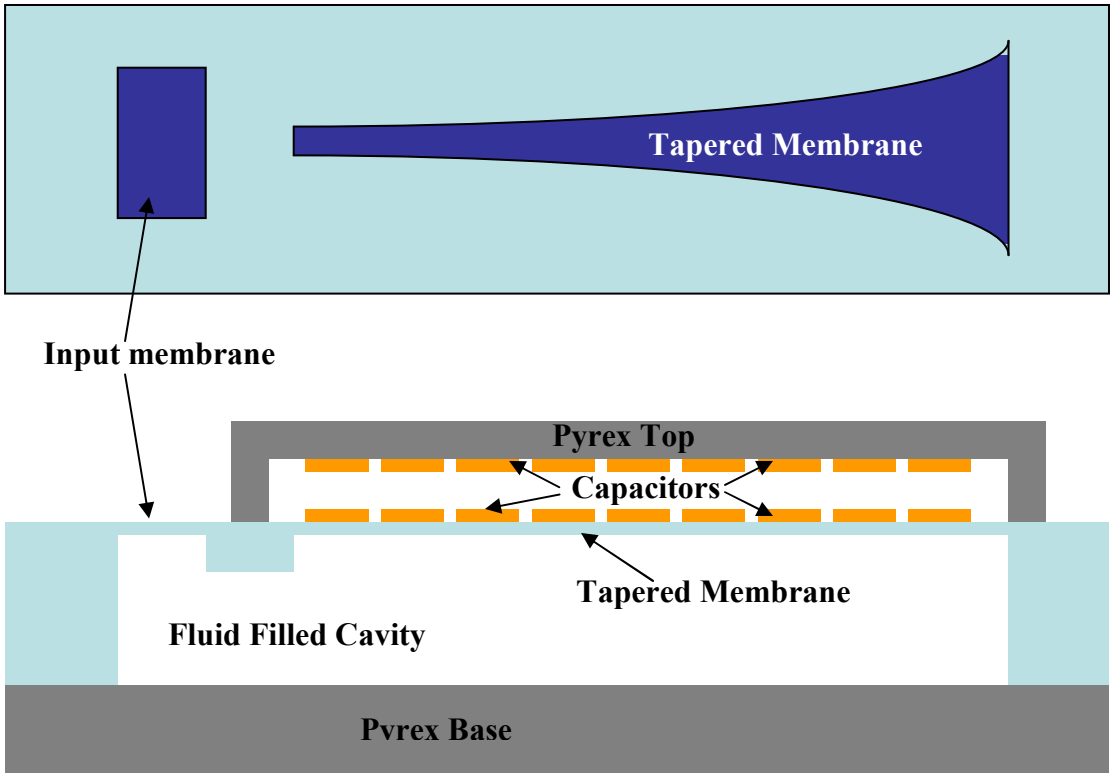

Figure 15. Figure adapted from [15] illustrating the cochlea base acoustic sensor.

Chapter 2: Underwater Packaging

2.1 Current underwater acoustic sensor packaging

Unlike typical microelectronic devices, acoustic sensors cannot simply be sealed off from the environment. Packaging for the device must protect it from the harsh underwater environment while allowing sound in. Moisture and salt ions can short electrical contacts and are a serious threat to reliability of an underwater sensor.

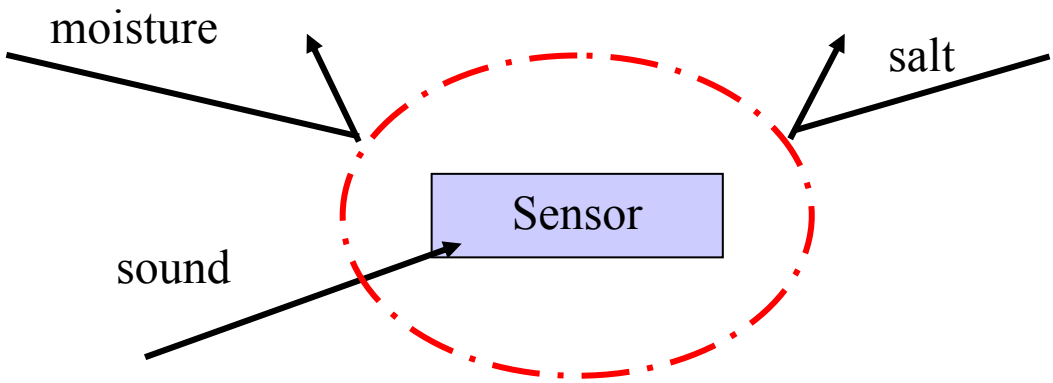

Figure 16. The package must be a barrier between the harsh environment while still allowing sound to pass through.

Devices such as the ones described in the previous section must allow sound to reach the sensing membrane or piezoelectric element. In the case of devices containing membranes, one side of the membrane can be exposed to the environment while the sensor's electrical contacts and other components can be safely sealed behind it. This is the approach taken by Bernstein et al. for packaging their devices [9,10]. As illustrated in Figure 17, the devices were bonded into Kovar flat-packs. A hole in the flat-pack allowed the bottom of the membrane to be in contact with the water environment. The top side of the device containing the PZT film, electrodes, and electrical connections were hermetically sealed safely inside the package.

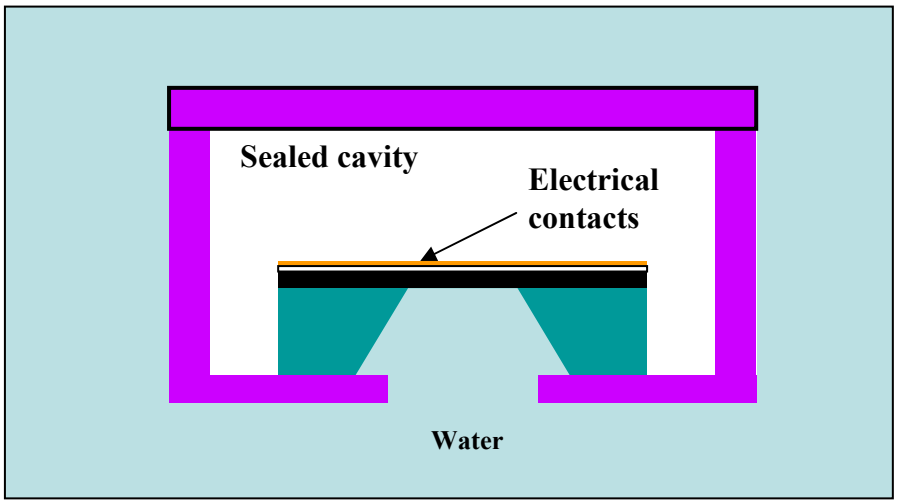

Figure 17. Water is allowed to reach the membrane through a hole in the flat-pack

Other devices that do not have moving parts can simply be encapsulated in an impedance matching encapsulant as is the case for the PVDF-MOSFET by Zhu et al. [13]. In that case a "Rho-c" rubber (they used a commercial polyurethane rubber) matching the acoustic impedance of seawater was coated on top of the sensor protecting it from the underwater environment while still allowing sound to penetrate.

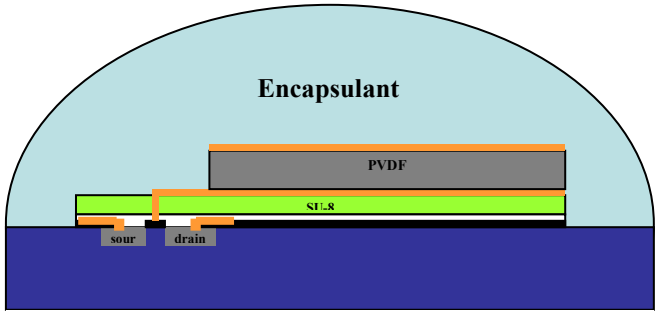

Figure 18. Encapsulation in a "Rho-c" rubber allows sound to reach the device while protecting it from the environment.

Phillip et al. also used "Rho-c" rubber as a passive underwater acoustic damping material [14]. In that application the material was combined with carbon fiber.

Sound enters the impedance matching material without reflecting acoustic waves back to the source and is absorbed by the other materials.

2.2 Packaging requirements for a nanowire acoustic sensor

The nanowire acoustic sensor poses unique packaging challenges that cannot be addressed using the methods described in the previous sections. Not only must sound be able to reach the sensor, but the nanowires must be free to move and interact with the sound waves. Furthermore, salt ions and moisture ingress will not only be detrimental to any electrical contacts within the package, it can corrode the nanowires causing a failure of the sensor.

Simply potting the nanowire sensor in a typical encapsulant was ruled out as option for protecting the sensor. That approach works well for sensors and transducers that are solid membranes or masses, but this would restrict the motion of the nanowires, adversely affecting the performance of the sensor. Another option would be to seal them in a standard hermetic package such as the Kovar flat-pack previously used. Since the delicate nanowires need to be protected from their environment, they would have to be positioned inside the hermetically sealed cavity. Though this would offer the greatest protection, sound cannot travel into the sealed cavity rendering the nanowires useless. Because of these challenges, a unique package design must be created to protect the nanowires while allowing sound to reach them.

Chapter 3: Design

3.1 Inspiration

Mammals use a complex system of membranes and bone structures to transfer sound waves to the sensing mechanisms inside their ears. The outer ear (the pinna and canal) collects sound and channels it to the middle ear while protecting the eardrum. The middle ear, consisting of the ear drum and three bone structures (the hammer, anvil, and stirrup), takes the sound (i.e. pressure waves in an air medium) and converts it into vibration of the bone structures. The end of the stirrup is connected to the base of the cochlea. Its vibration causes a pressure wave inside the fluid of the cochlea.

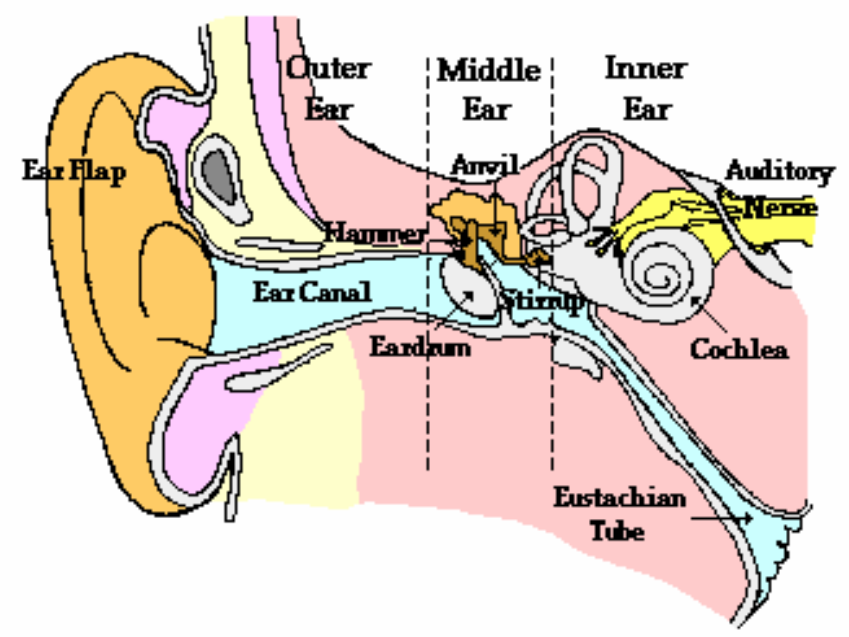

Figure 19. A drawing of the organs in the human ear [17].

Inside the cochlea, the cilia along the basilar membrane sense its movement and send signals to the auditory nerves. The sensor developed for this study uses nanowires that mimic these cilia and will also operate inside a fluid medium to allow their

movement. A major difference between the human ear and the nanowire sensor is that the sensor is being packaged for underwater applications. The human ear has a functional package that physically transfers the sound from air to liquid. Because the nanowires sense sound that is already in water, another biological analogy was made to fish. Figure 20 shows hair cell bundles inside a lizard fish.

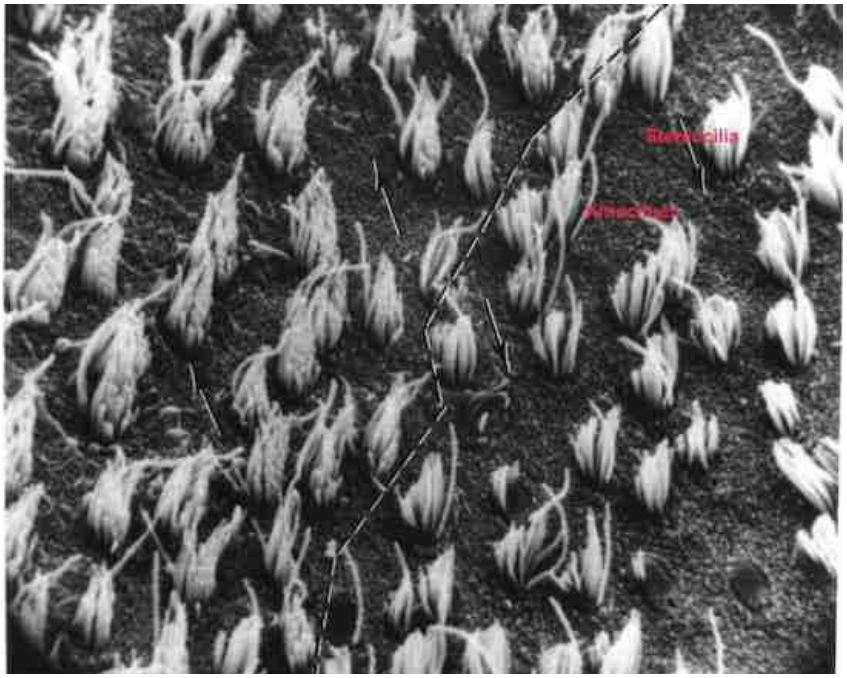

Figure 20. Ciliary bundles from a lizard fish [18].

Fish and other aquatic animals are required to sense acoustic waves that are already traveling in a liquid medium. These animals hear by allowing sound to pass through their bodies. The sound waves are transferred from the water through the tissues of the fish to their sensing organs, which are stimulated by the sound wave interaction [19]. This works because the tissues that make up the body of the fish have an acoustic impedance match to the water environment and allow sound to pass. Based on this example, this package uses impedance matched materials to allow sound to

pass through the package to reach the Galfenol nanowires. The goal is to select the proper materials and incorporate them into a package design.

3.2 Package layout

The package design seals the nanowire sensor inside a fluid filled cavity. The fluid medium allows the nanowires to move and respond to incoming sound waves. The cavity is sealed off with a window made from an acoustically transparent material. Both the window material and the filler fluid must have an acoustic impedance match to seawater allowing sound to pass through and interact with the nanowire sensor. An early design, shown in Figure 21, illustrates the idea of sandwiching the sensor between two acoustically transparent windows.

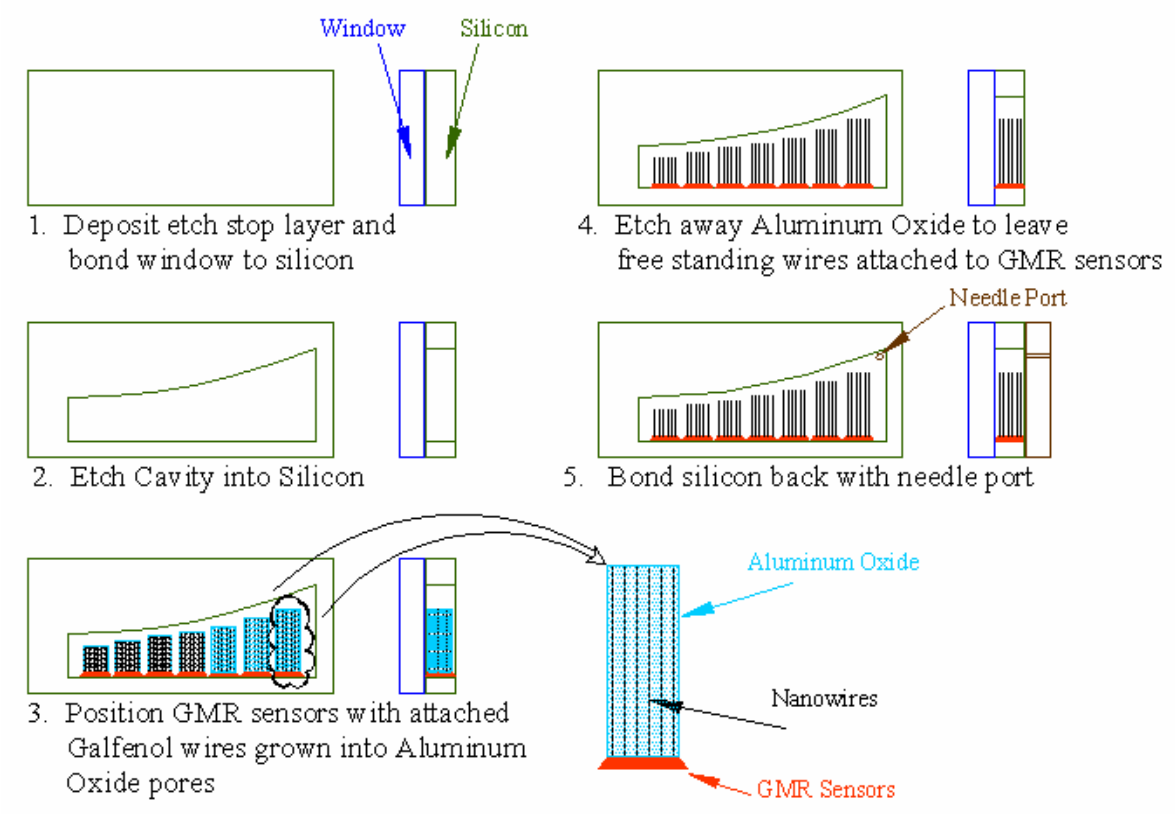

Figure 21. A schematic showing an early design and fabrication steps for a possible package layout.

Problems arose while examining the feasibility of constructing such a package. First, the drawing shows the nanowire sensor being bonded to the edge of a through-hole in a silicon wafer. While the scale of the nanowires themselves would permit them to fit on this 550 µm edge, physically bonding the nanowire array and a GMR sensor in this position would be difficult. Second, early prototypes of the sensor will surely be larger than 550 µm wide. Preliminary samples of nanowire arrays measure about 1 cm by 1 cm and GMR sensor chips such as the one shown in Figure 2 measure about 2 mm x 5 mm. Figure 22 shows a Galfenol nanowire sample grown at the University of Minnesota. The alumina template is glued onto a silicon wafer for handling purposes. The white area is the bare template and the blue area is where the nanowires are grown into it. The nanowires are only grown onto the part of the template that had the copper electrode printed on the back. A template similar to this one must fit inside the package.

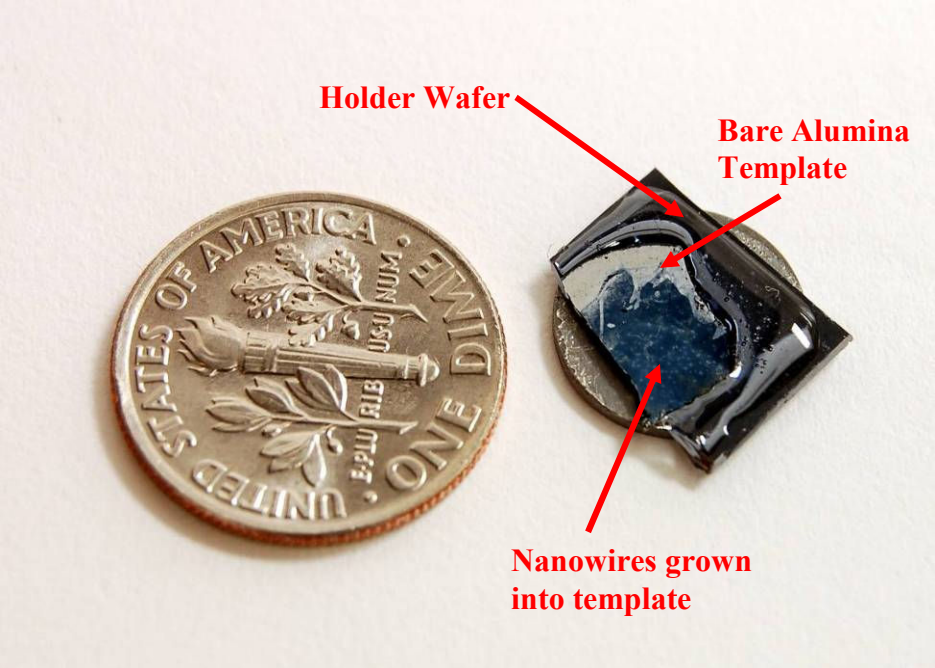

Figure 22. An alumina template on a silicon holder wafer. The white area is part of the alumina where nanowires were not deposited and the blue is where nanowires were grown.

As a result, this early configuration was abandoned, and one that offers more flexibility in the size of the nanowire sensor was adopted. The new design, illustrated in Figure 23, shows the nanowire array bonded to the surface of a cavity that is etched down into a silicon substrate. By doing so, the dimensions of the cavity can be easily changed depending on the height and area of the nanowire arrays and GMR sensors.

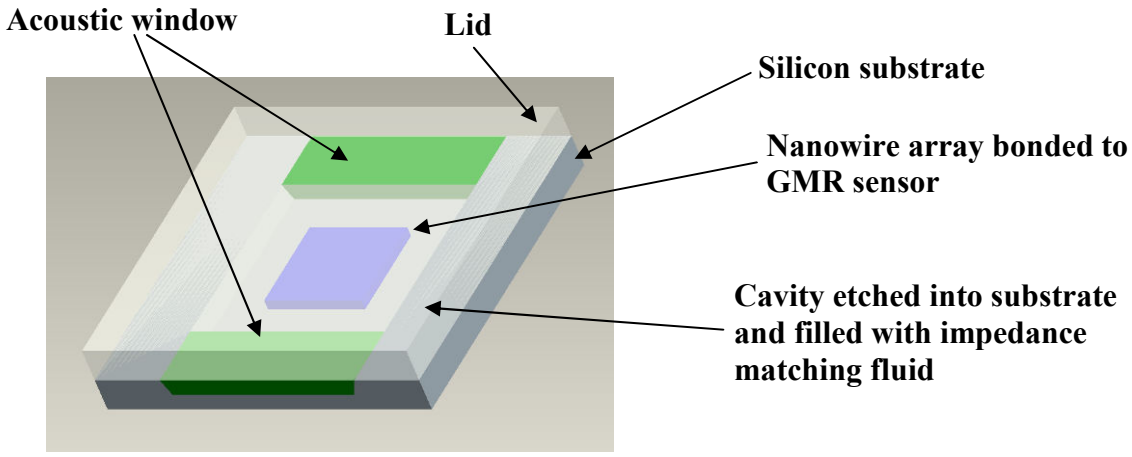

Figure 23. A drawing of the package with the components labeled.

A sealed cavity containing the sensor and impedance matching fluid must be fabricated. The structure needs to incorporate the window material to allow sound to reach the sensor. A cavity is etched into the surface of the silicon substrate. Silicon was chosen for cost as well as the wide variety of etches available for creating the cavity. A glass lid bonded to the substrate seals the top of the cavity creating a channel with two open ends. An advantage of glass is that the inside of the package can be seen to ensure that all air is removed before sealing. The acoustic window material molded into the ends will seal the cavity. The side view shown in Figure 24 illustrates how sound will reach the sensor.

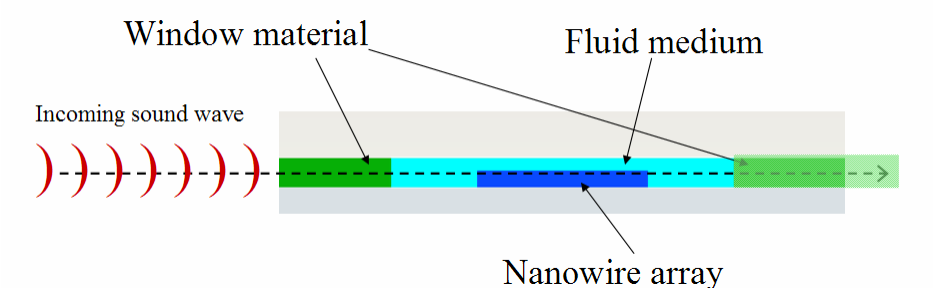

Figure 24. A side view of the package showing the direction of sound propagation.

3.3 Material selection

The success of the package depends on the proper selection of materials that, when used together, will allow sound to reach the nanowire sensor while protecting it from the harsh underwater environment. Materials matching the acoustic impedance of seawater must be found for the acoustic window and fluid medium. A minimal difference in impedance will result in low signal loss due to reflections at the material interfaces. Acoustic impedance (Z) is a function of the material's density (ρ) and the acoustic wave speed (c) within the material as shown in (1). The reflection coefficient (R) for a sound wave traveling from one material to another is shown in (2). Though the acoustic impedance may be matched for two materials, it is still necessary to specifically match the wave speed within the two materials to avoid loss from the angle of incidence of the incoming acoustic wave [20].

$$Z = \rho \cdot c \tag{1}$$

$$R = \frac{Z_2 - Z_1}{Z_2 + Z_1} \tag{2}$$

A scanning acoustic microscope (SAM) was employed to find the acoustic wave speed for various potential materials. There are other methods available for finding the acoustic wave speed in media such as using a commercial ultrasonic thickness gauge. Such devices are typically used to measure the thickness of pipes or other objects that are difficult to measure by conventional means. They work by sending an acoustic pulse through a sample. The device measures how long it takes for the pulse reflection to reach back to the transducer. Using the known acoustic wave speed in the material, the thickness is calculated. The goal of this study is to do the opposite: measure the how long it takes for the reflection to come back to the transducer and use the known thickness to calculate the wave speed. The SAM available at our laboratory facilities can be used in this manner and was selected for the task rather than purchasing a piece of equipment.

Tests were performed in a SONIX scanning acoustic microscope. This sophisticated piece of equipment is traditionally employed to do non-destructive analysis on die attaches and other joints. It can produce an image that will represent voiding or cracking between two bonded components. In its most simple mode of operation, it will send an acoustic pulse at the sample and record any reflections sent back at the transducer. The reflections occur at material interfaces where differences in the acoustic impedance of two materials will cause some acoustic energy to be transmitted and some reflected.

A setup is required to hold a layer of material at a constant known thickness for the test. The fluid for the filler material was sealed between a glass bottom and plastic lid (Figure 26), A standard glass microscope slide was used as a spacer to keep the thickness of the sample constant. The slide thickness was measured with calipers and found to be 1.1 mm thick. The setup was then placed under the SAM transducer. A first attempt at fabrication used a glass lid instead of plastic. The trace from the SAM transducer showed that the sound did not penetrate the glass slide and no discernable reflections could be identified. In Figure 25, the top shows the trace from the sample with a glass lid. The pattern of the trace is characteristic of the sound wave hitting the glass slide.

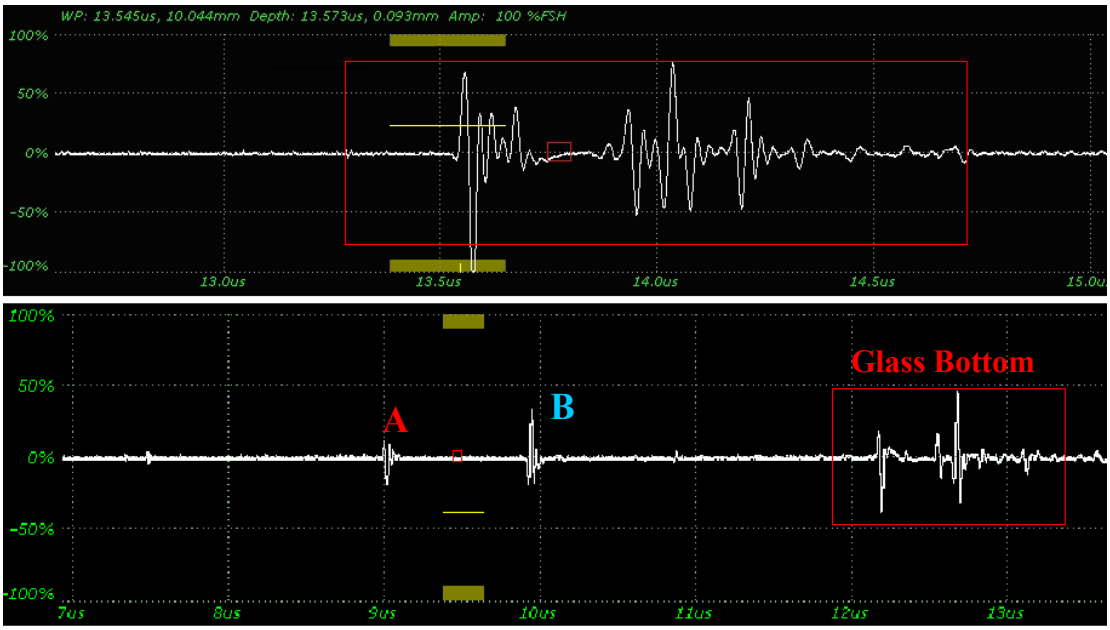

Figure 25. Top: A trace from a sample with a glass lid; Bottom: A trace from a sample with a plastic lid.

The trace on the top matches the part of the trace boxed on the bottom of Figure 25 when the acoustic wave hit the glass bottom of the test setup that used a plastic lid instead of a glass one. Reflections A and B are from the top of the plastic lid and the top of the sample material respectively. Once the glass lid was replaced with the

plastic one, three clear reflections could be seen on the SAM output. Figure 26 shows the layout of the setup. Reflection A, B and C are marked and correspond to those labled in Figure 26. The time between reflections B and C (marked in Figure 27) was measured using the SAM output and equation (3) was then used to calculate the wave speed.

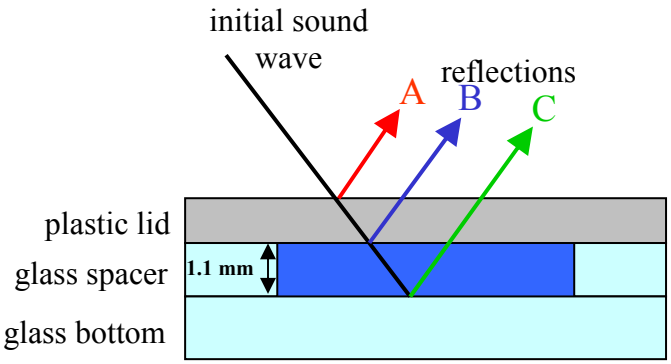

Figure 26. A drawing of the SAM testing setup.

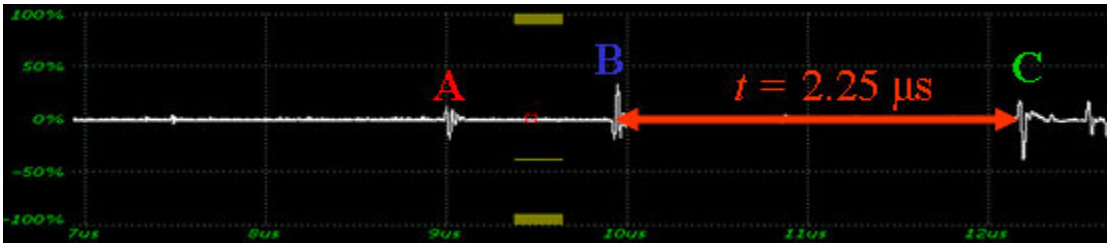

Figure 27. An SAM output for the testing setup filled with a silicone oil.

$$c = \frac{2 \cdot (.0011m)}{t[\text{sec}]} \qquad (3)$$

Several different fluids and encapsulation materials were investigated for possible use in the package. Standard dielectric fluids were chosen as potential filler fluids, including silicone oil, ethylene glycol and castor oil. To verify the experimental procedure, materials with known properties were tested first and the values were compared to those found in literature. The speed of sound in DI water was measured

to be 1495 ± 10 m/s, which matches the reference value for water at 23 ºC [21]. The error associated with the measurement comes from graphically determining the time between the two reflections. The value could only be determined within 0.05 μs.

Two different silicone rubbers were tested with the setup as well as a polyurethane rubber. All silicone and polyurethane samples were mixed and cured as per manufacturer's instructions. The first silicone rubber was GE Silicone's RTV-615, which is a two part mixture. It was chosen because it is a typical silicone encapsulant used for protecting electronic components from moisture, shock and vibration. Ten parts of the "A" component were mixed with one part "B". The two ingredients were mixed thoroughly in a cup with a stirrer. The mixture was degassed under vacuum for ten minutes to remove all air bubbles. The mixed encapsulant was then poured onto the glass slides of the test setup and the lid was clamped in place so that a constant thickness sample was made. RTV-615 can be cured at room temperature for 7 days or at 150 ºC for 15 minutes. The later was used for the samples that were tested.

The second silicone rubber tested was GE Silicones' RTV-6126, which is used for the same purposes as RTV-615 but is much softer. It was chosen in contrast to RTV-615 to see if a softer rubber would have substantially different acoustic properties. RTV-6126 is mixed from equal parts of the A and B components. It is mixed and degassed the same way as RTV-615, but cures much quicker. It cures in less than one hour at room temperature.

The polyurethane rubber selected was RenCast 6400-1. One part of the resin was mixed with ten parts hardener for ten minutes. The uncured mixture has a low enough viscosity that it did not require degassing. The rubber cures in 6 to 7 days at room temperature.

The wave speed and density were obtained by SAM for each candidate and compared to water and seawater as shown in Table 1. The closest matches found were castor oil for the filler fluid and polyurethane rubber for the window material. Polyurethane rubber and castor oil have measured acoustic impedances of 1.56 and 1.43 respectively. Seawater's room temperature acoustic impedance is 1.56 [**21**]. Both materials were chosen for further investigation. Further investigation will focus on whether these materials are compatible with the fabrication of the package and reliable in the underwater environment.

Table 1. Room Temperature acoustic properties of investigated materials.

Material	**Density (g/cm^3)**	**Wave Speed (m/s)**	**Impedance (rayl x 10^6)**
Water (20ºC) [**21**]	1.000	1483.2	1.48
Seawater (20ºC) [**21**]	1.028	1522.2	1.56
DI water (measured)	1.00	1495	1.50
Silicone oil	0.96	980	0.94
Ethylene Glycol	1.12	1660	1.86
Castor Oil	0.969	1490	1.43
Silicone Rubber A	1.02	1080	1.10
Silicone Rubber B	1.05	1030	1.08
Polyurethane Rubber	1.04	1500	1.56

Chapter 4: Fabrication

4.1 Fabrication of the package base

The following process sequence describes the procedure for fabricating the prototype package:

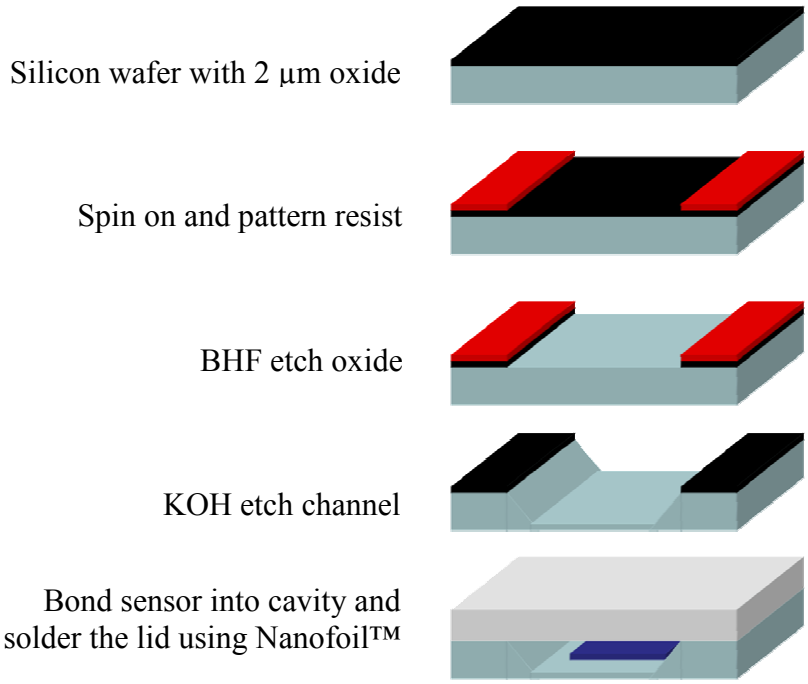

Figure 28. An illustration of the process sequence with the steps labeled.

For the substrates, a single side polished 1-0-0 silicon test wafer with 2 µm thermally grown oxide from Isonics, Inc. was used. Shipley 1813 photoresist was spun on at 3000 rpm for 30 seconds, then soft-baked for 1 minute on a hotplate at 100 ºC. The resist was exposed under a transparency mask in an Oriel aligner and developed for 30 seconds in Shipley 352 developer. The mask for the substrate (shown in Figure 29) defined the etched channels as well as smaller etched lines that define the edges of each package base. These etched lines were included in the design for two

reasons. First, the channels have a desired depth of 250 µm. By making the width of the lines 350 µm, the v-groove created will have a self-limiting etch stop at the desired depth of 250 µm. A microscope was used to examine the v-groves periodically during the etch, and the etch was stopped after the v-grooves were determined to have self limited. Second, the wafer did not need to be diced after etching because the package would easily break free from the substrate along the grooves.

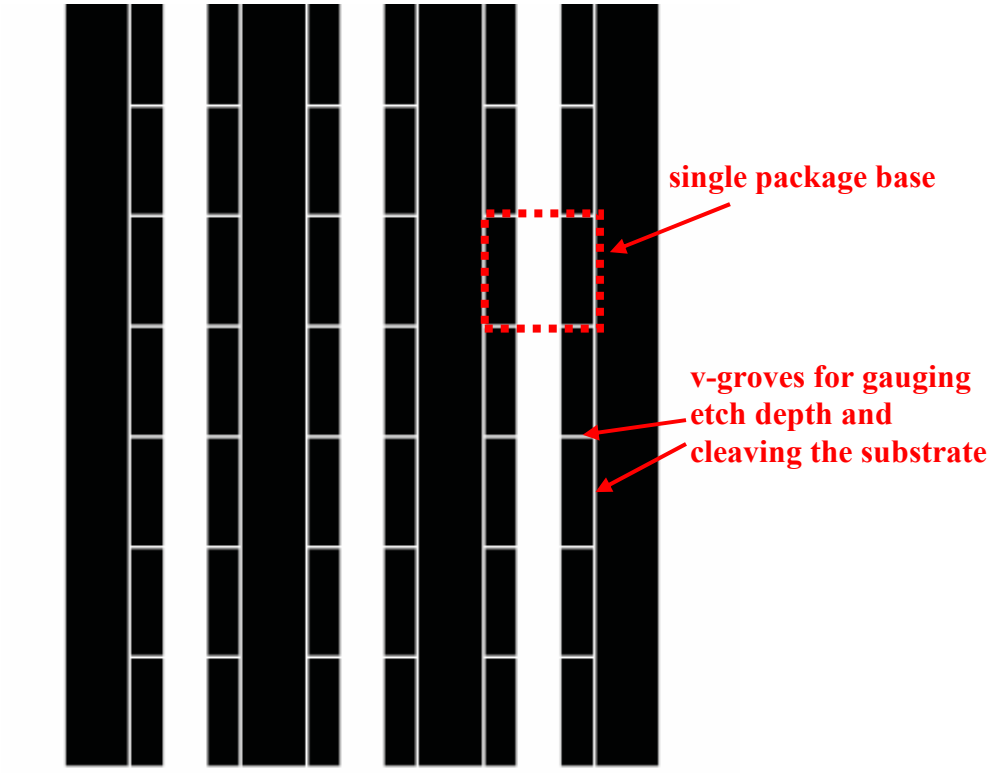

Figure 29. A drawing of the mask used to define the etched channels and package outlines.

Once the resist had been patterned, the oxide was etched in BHF from Transene. Etch rates of about 0.1 µm per minute were measured for the oxide. Measurements were made by removing the wafer from the BHF, rinsing and drying them, then measuring the etch depth on a Tencor profilometer. Wafers were then put in a 35 wt% KOH

solution prepared from KOH flake. The solution was heated to 85ºC on a programmable hotplate with temperature probe and stirred with a 1" stir bar at 250 rpm (setup shown in Figure 30).

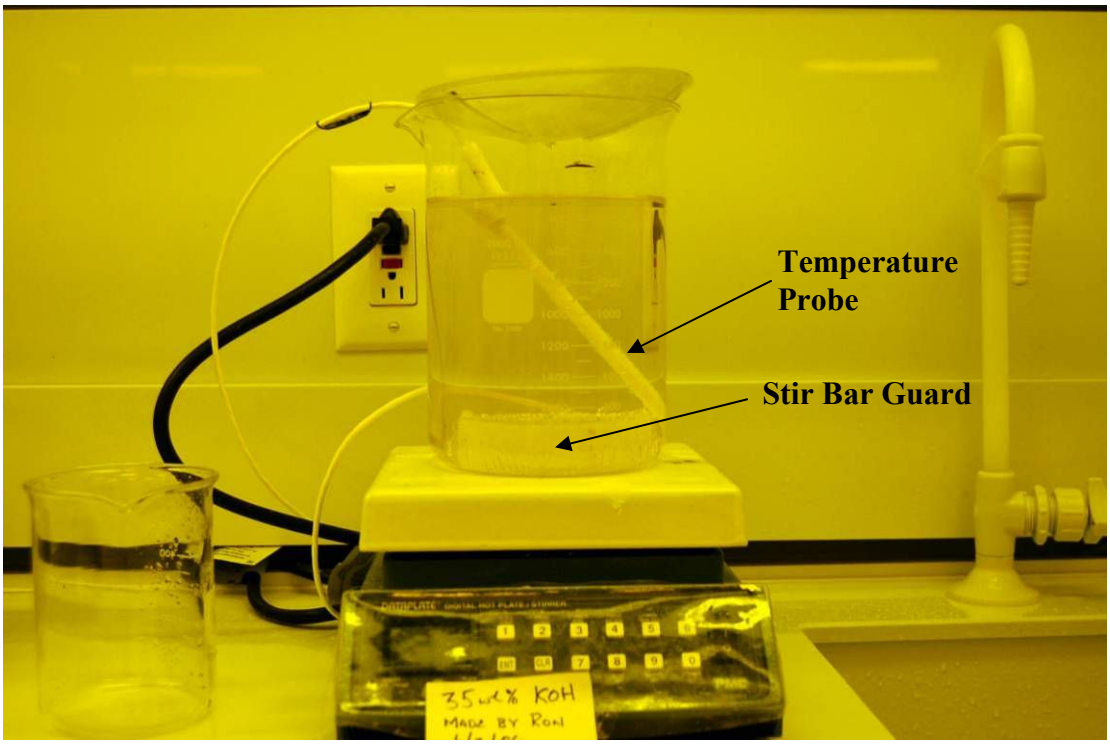

Figure 30. KOH etch setup.

Etch rates in the KOH solution were measured to be about 70 µm per minute. After the etch depth reached 250 µm, the wafers were removed from the solution, rinsed and dried. The remaining oxide was removed with BHF. Figure 31 shows a wafer after being removed from the KOH etch.

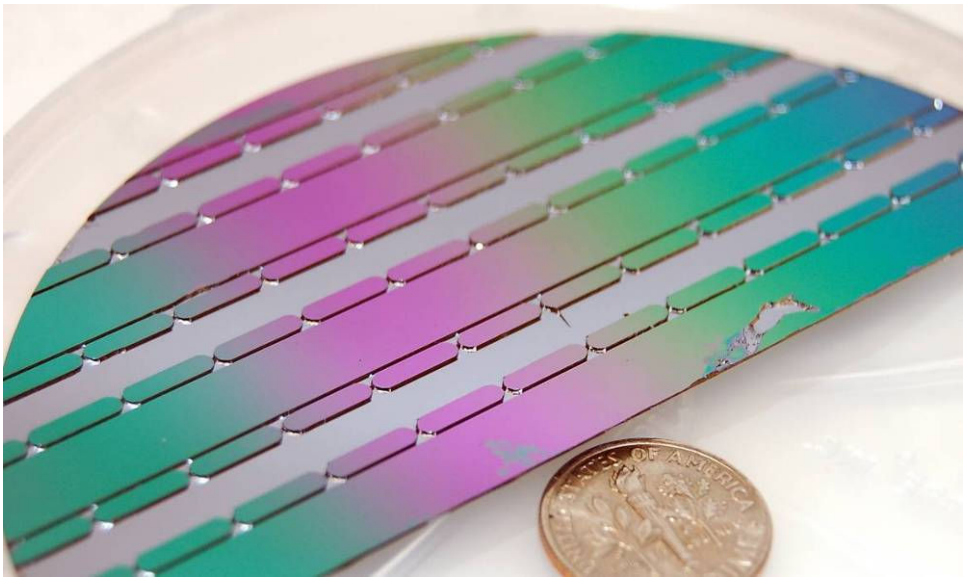

Figure 31. A half wafer after removal from the KOH etch and before removal of the oxide.

4.2 Package assembly and room temperature soldering

Several methods were investigated for bonding the glass lid to the silicon substrate. Anodic bonding was initially tried. Several test bonds were performed using the EVG bonder. The silicon and Borofloat™ wafers were brought up to 300 – 400 ºC and a 900 V bias was used. The bonding process including heat up and cool down took 2 – 3 hours on average. The success of the bond depended heavily on the effectiveness of the RCA cleaning process done prior to bonding. Many small voids were observed presumably where contaminant remained on the wafer surface. Anodic bonding was not explored further because the high temperatures required could cause damage to the GMR sensor, nanowires, or any other bonding material previously used in the fabrication.

A room temperature soldering process using Nanofoil™ from Reactive Nano-Technologies was attempted for the bonding. NanoFoil™ contains multiple

alternating nano-layers of aluminum and nickel. Ignition of the foil starts a self-propagating exothermic reaction, which provides enough thermal energy to melt the solder without significantly raising the temperature of the two components being joined. Such a method has been shown to produce hermetic sealing of stainless components [22]. In this application, the surfaces were coated with Cr-Au metallization to enhance solder wetting. Indium solder ribbon (1 mil thick) was chosen as the solder, because it had been shown to work in hermetic sealing applications [22]. It is also ductile and wets well to gold metallization.

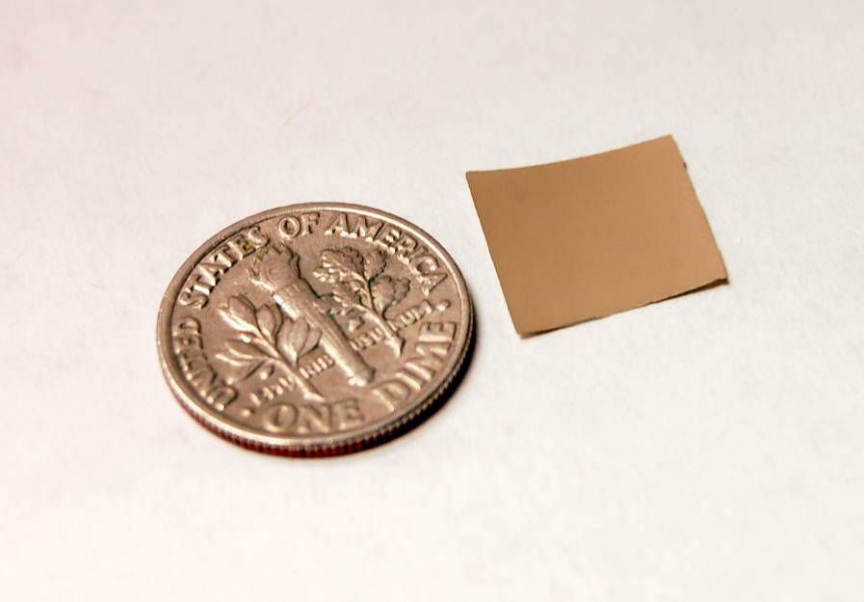

Figure 32. A single 0.5" x 0.5" piece of 60 µm thick Nanofoil™.

To create the solder joint, a 60 µm thick piece of NanoFoil™ is placed between two solder performs. The three layers are then sandwiched between the two surfaces to be soldered as shown in Figure 33. In this case it was the metallized lid and substrate. A 0.7 MPa pressure is applied to the stack with a weight, and the foil is ignited. For ignition, two leads attached to a 9 V battery were touched to the edge of the

NanoFoil™. The bonds created for the package could not be broken apart without first breaking the silicon substrate or glass lid.

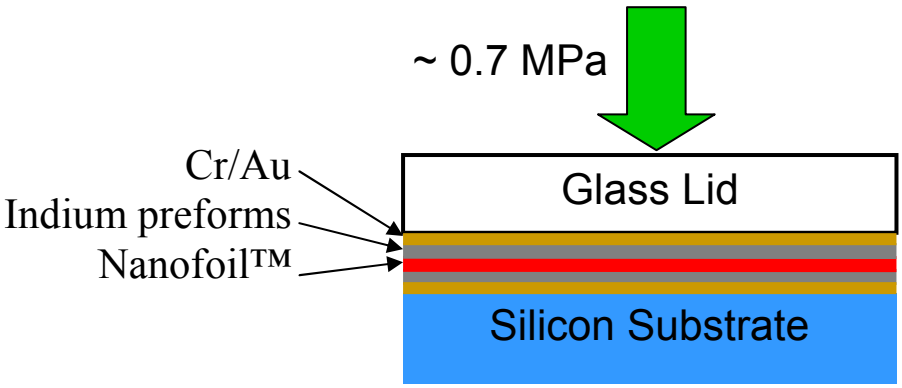

Figure 33. A drawing of the components in the bonding process.

Cleaving of the wafer into individual package bases (shown in Figure 34) was done using tweezers. The wafer broke cleanly along the etched v-groves with little effort. To implement the room temperature soldering process, etched silicon wafers (shown in Figure 31) as well as Borofloat™ glass wafers had Cr/Au metallization evaporated onto them. The glass wafers were diced into lids for the packages that were attached using NanoFoil™ and indium solder preforms. The bonded lids and bases were then ready to have the polyurethane windows molded into place.

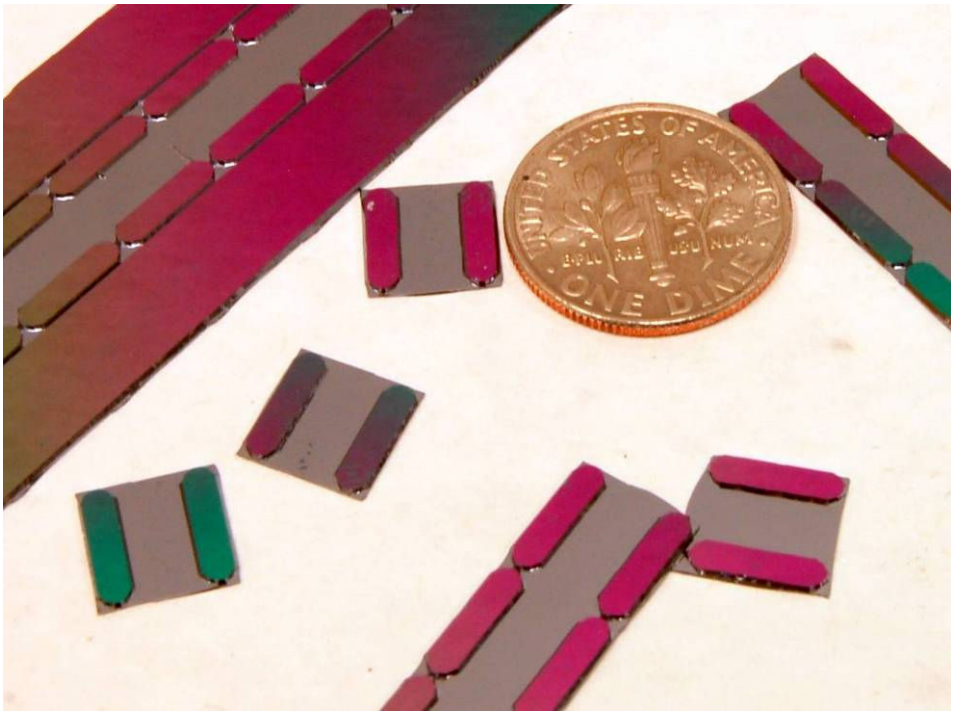

Figure 34. Individual package substrates after being cleaved from the half wafer.

4.3 Acoustic window molding

In order to investigate the logistics of molding the windows several packages were assembled using an epoxy to bond the lid and base instead of the Nanofoil™ and solder. Figure 35 shows several packages held up by copper wires.

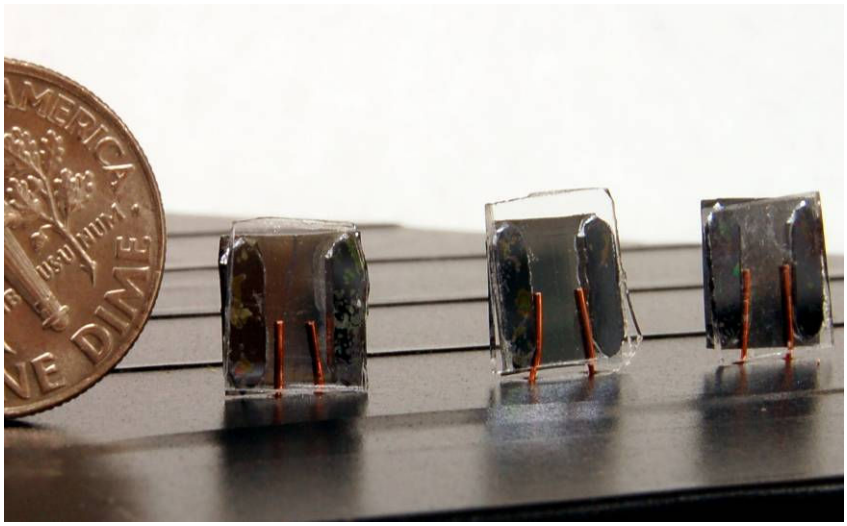

Figure 35. Assembled packages ready for molding.

The packages were held vertically by wires that were inserted though holes in a taped plastic sheet. RenCast 6400-1 polyurethane rubber was made by mixing one part of the amber resin with ten parts of the off-white hardener. The two components were weighed on a digital scale, combined, and mixed vigorously stopping several times to scrape down the sides of the container. After mixing was completed, some polyurethane rubber was placed at the bottom of the package. Capillary forces pulled the polyurethane rubber up into the channel. The viscosity of the mixed rubber immediately after mixing is low enough that the capillary forces pull the rubber up until it fills the entire cavity (shown in Figure 36), which is undesirable.

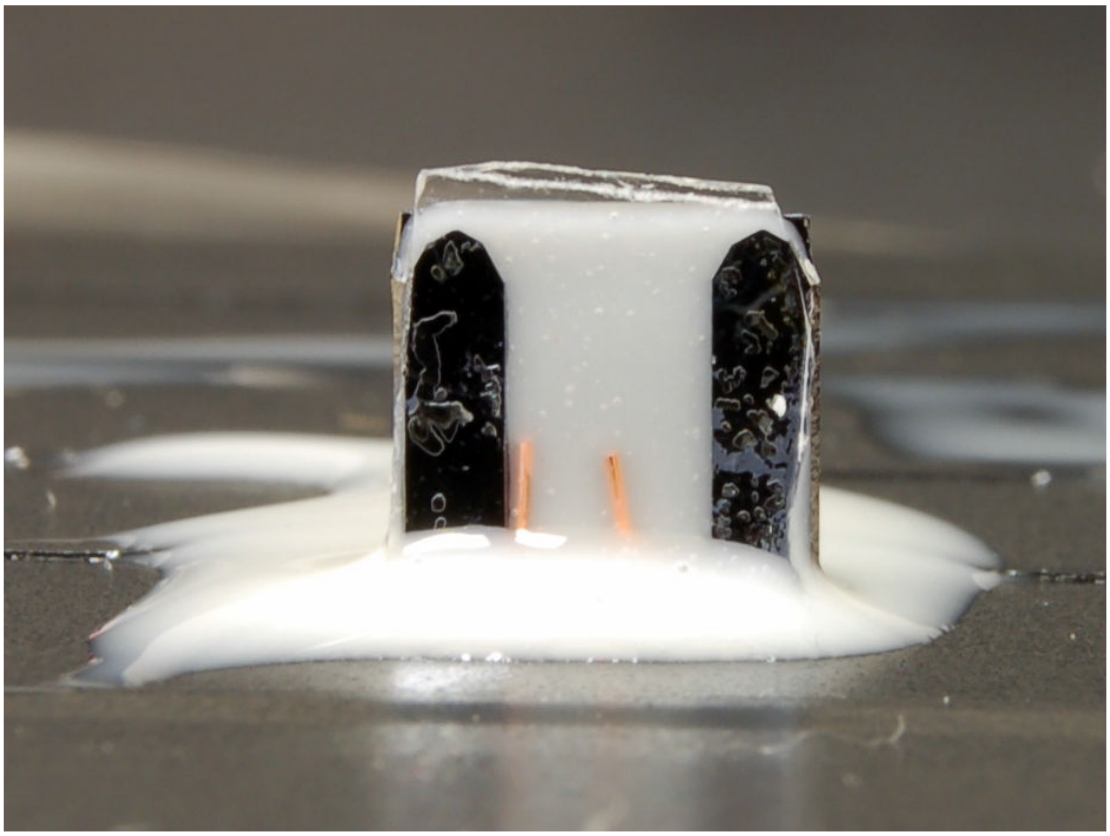

Figure 36. A package filled completely with polyurethane rubber.

To solve this problem, the rubber was allowed to set before it was applied to the package. The rubber was applied to several packages in increments of 3 minutes set time in order to determine the optimum set time. Figure 37 shows that allowing the polyurethane to set between 6 and 9 minutes allows the viscosity to increase enough so that the capillary forces will not pull it too far into the cavity.

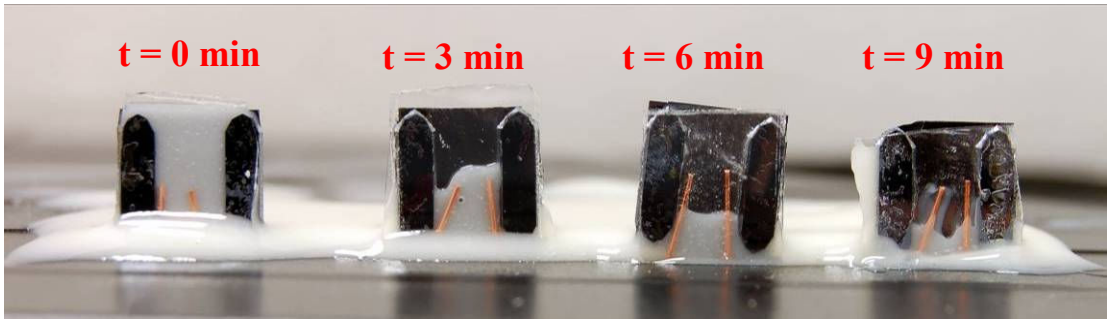

Figure 37. Packages with polyurathane molded at different set times.

Once the window is molded into one end of the cavity, the packages are filled with castor oil. Again, capillary forces dominate and the castor oil is pulled into the cavity. Only one corner was submerged in the oil to allow air to escape. After filling, the entire package was placed into a final polyurethane over-mold, completely sealing the cavity (Figure 38).

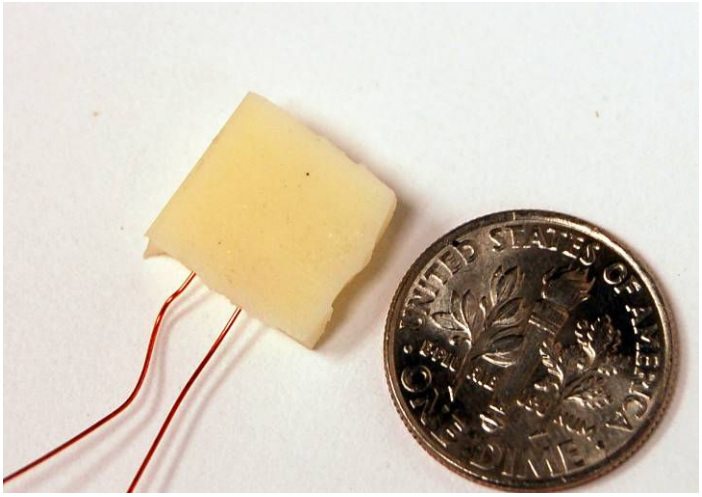

Figure 38. A package after final molding in polyurethane.

Chapter 5: Testing

5.1 Acoustic Tests

To verify that the castor oil and polyurethane rubber work well together as impedance matching materials, a test package was designed and fabricated. The goal of the test package was to use castor oil and polyurethane to package and protect a commercial microphone and compare its performance to an unpackaged microphone. For the commercial reference microphone, a miniature waterproof microphone from Knowles Acoustics (Part # WP-3501) was purchased. This microphone was chosen for its size so that the test package could be as small as possible, and, because it is waterproof, so it could be used as both the packaged microphone and the reference microphone. The first test package was designed to hold the microphone in a stainless steel housing. Type 304 stainless steel was used because the size of the microphone did not permit it to be placed in the silicon packaging. Stainless steel was chosen for its corrosion resistance and because it is also compatible with the Nanofoil™ soldering process [22]. A base and top were machined to create a channel to hold the microphone. After machining, the bond surfaces were polished on a polishing wheel to remove scratches and imperfections. Then Ni/Au metallization was evaporated onto the bond surfaces. The two parts were bonded using the same NanoFoil™ described in the previous chapter. This resulted in a solder bond that did not require high temperature reflow.

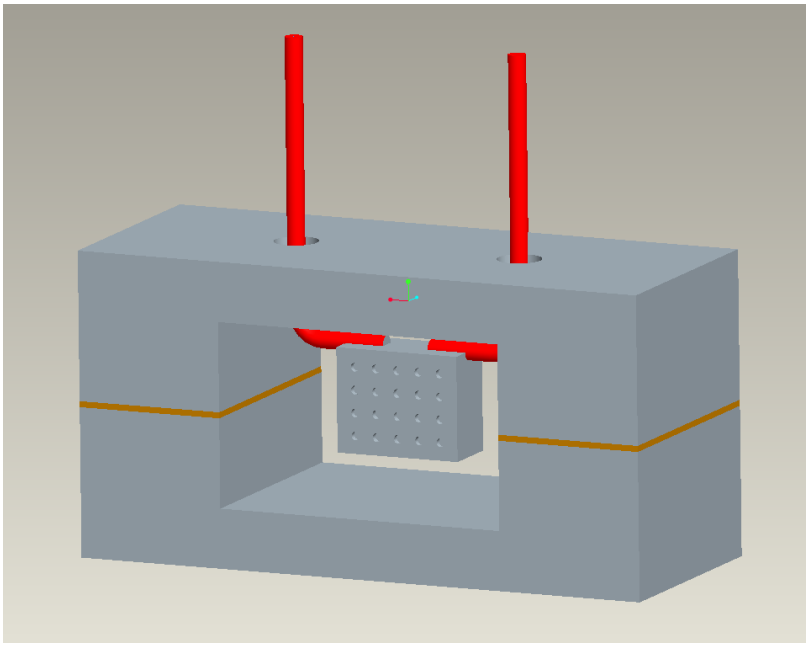

Figure 39. A CAD drawing of the acoustic test package assembly before molding.

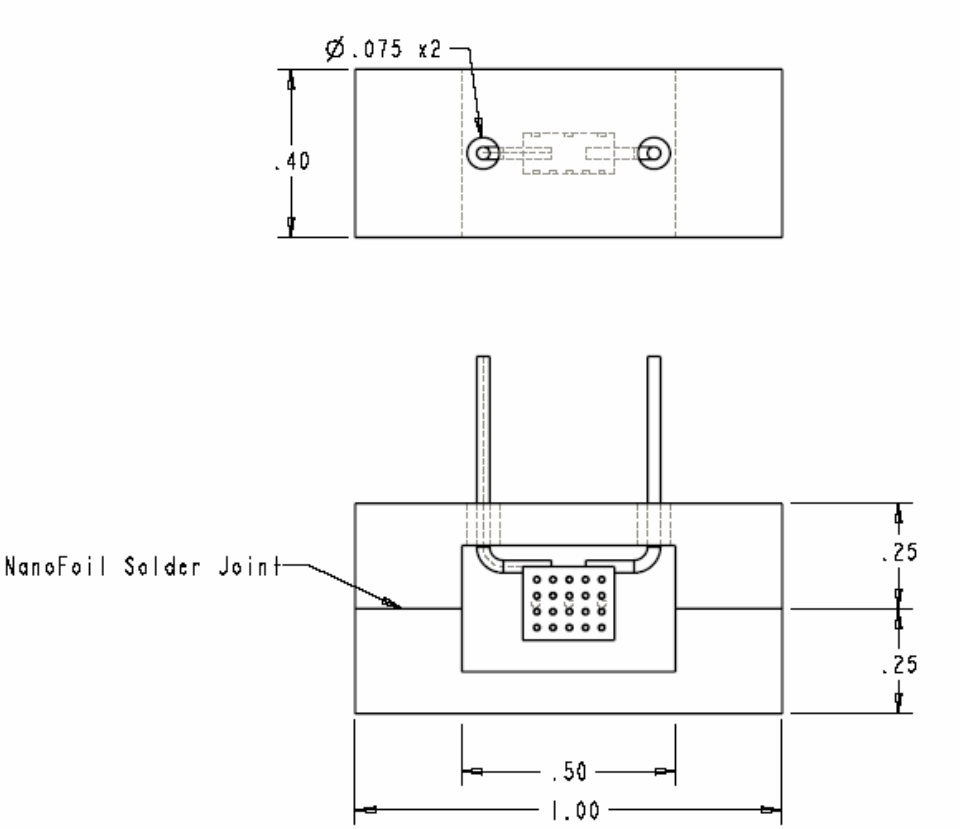

Figure 40. A drawing of the acoustic test package showing relevant dimensions

In order to seal the cavity with polyurethane rubber and fill it with castor oil, several molding steps were performed. First, thin windows were molded on each end of the channel. Once both windows had set and cured, one was peeled off. Figure 41 shows a picture of the test package at this stage. The cavity was then filled with castor oil and the window was carefully replaced making sure to allow all air and excess castor oil to escape the cavity. With the window firmly in place, the assembly was wiped clean with acetone. The polyurethane does not adhere well enough to stainless steel to provide an adequate seal. As a result, the assembly was placed in a larger mold and over-molded to completely encapsulate the package.

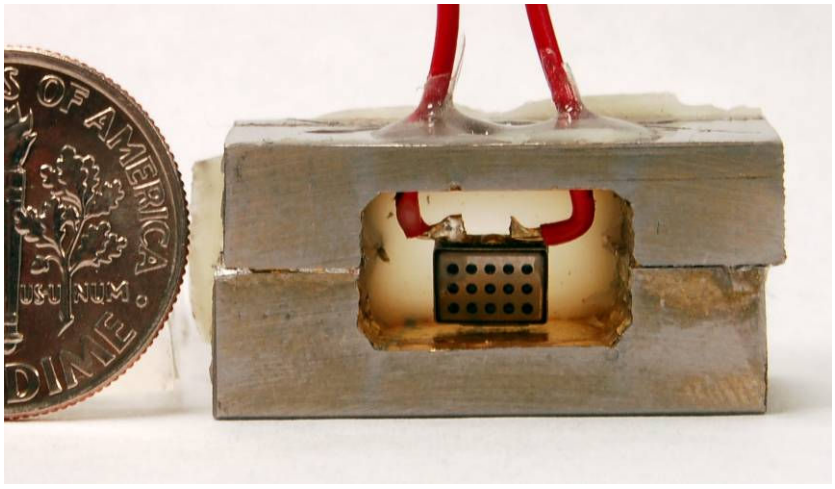

Figure 41. A picture of the stainless steel test package with the WP-3501 microphone before over-molding. The front window was removed and the picture was taken before the cavity was filled with castor oil.

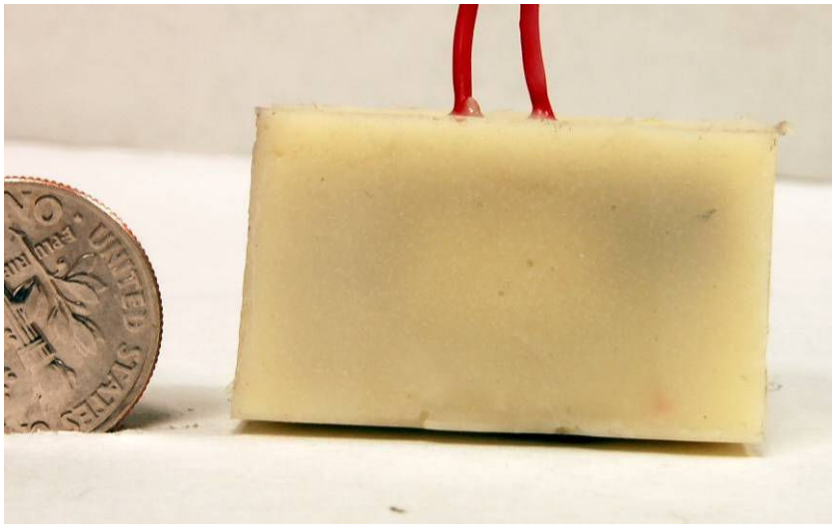

Figure 42. A picture of the package after over-molding.

For reasons discussed later in the section, a second test package was designed and fabricated. This second package did not contain a stainless steel housing to hold the microphone. A base and lid were molded entirely out of polyurethane so that there would be no effect on performance by the metal structure. Polycarbonate molds were fabricated to mold the base and lid, which were fabricated such that the leads to the microphone could be fed through during molding. Once the base was molded it was filled with castor oil, and the lid was sealed on with epoxy. Last, a final over-molding with polyurethane was conducted (Figure 44).

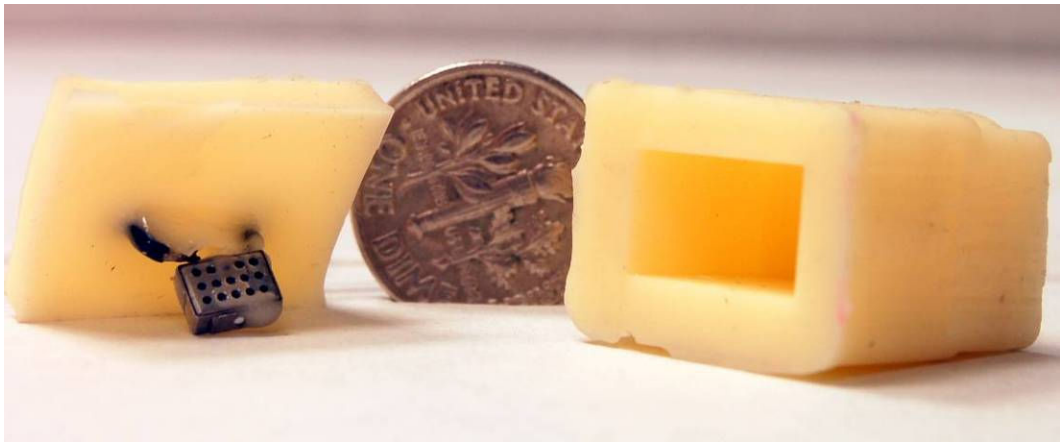

Figure 43. The lid and base for the all polyurethane package. Note the Knowles WP-3501 microphone molded into the lid.

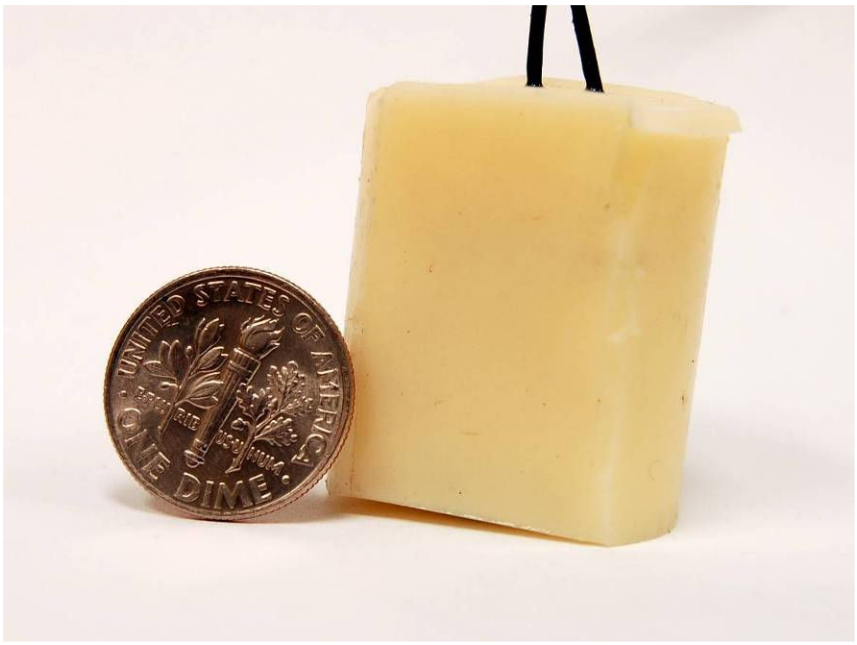

Figure 44. The over-molded all polyurethane package.

The acoustic test setup consisted of a 15 gallon glass tank with an aluminum plate epoxied to the outside of one wall. The plate had a threaded hole so that one end of a Terfenol transducer could be attached. The other end of the transducer was bolted to another plate and clamped to a cinderblock used as a counter mass. Figure 45 is a picture of the test setup with the components labeled.

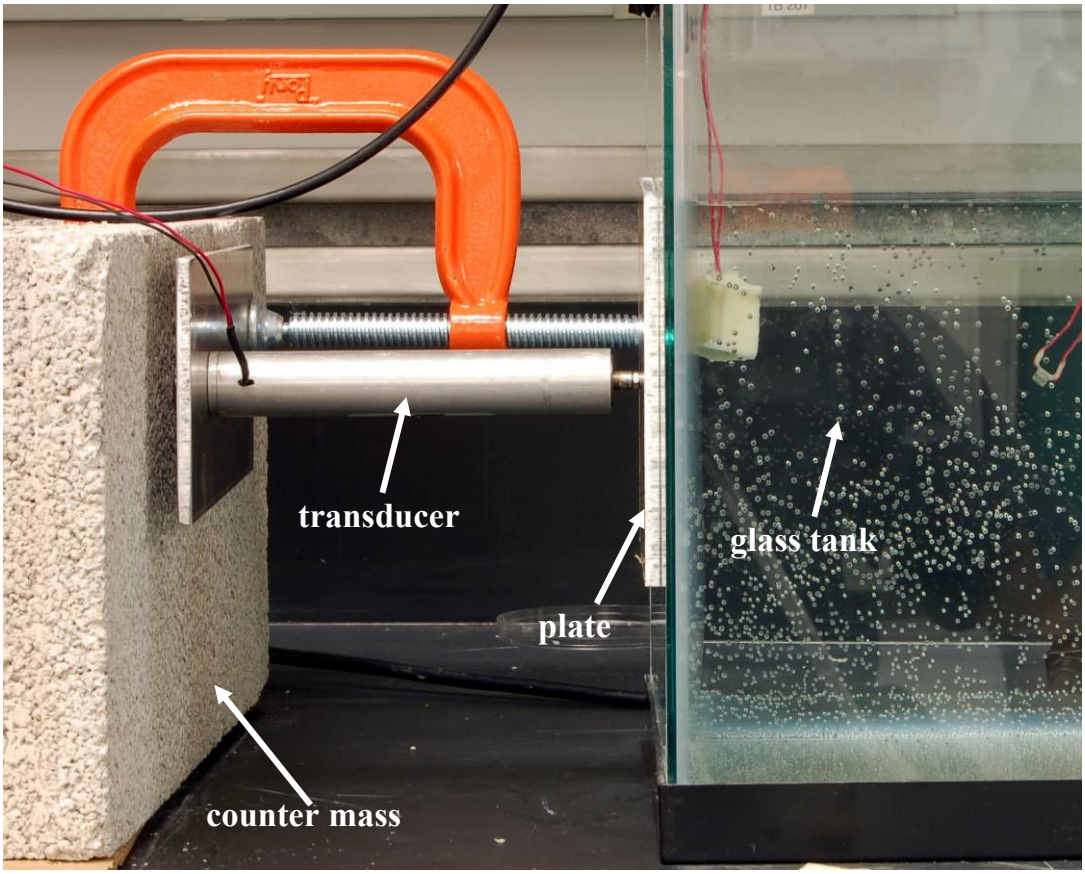

Figure 45. The acoustic test setup with components labeled

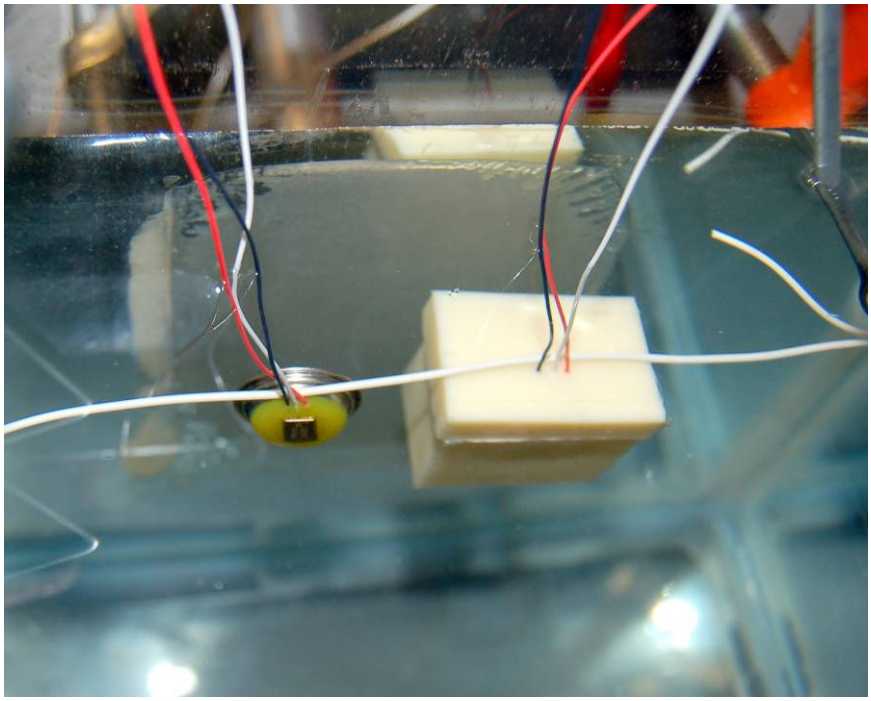

Figure 46. The unpackaged packaged (right) and packaged microphone in the test tank.

Wires were strung across the inside of the tank to hold the packaged and reference microphones an equal distance (2 inches) from the wall (Figure 46). Holding the microphones far from the wall (in the center of the tank) decreased their output. The transducer was driven at a range of frequencies with an Agilent function generator. The signal was amplified with a linear amplifier. Data was taken with an Agilent digital oscilloscope (equipment shown in Figure 47). The circuit in Figure 48 was obtained from the microphone data sheet and was used to power the microphone and monitor its output.

Figure 47. The Agilent function generator (right) and digital oscilloscope (left).

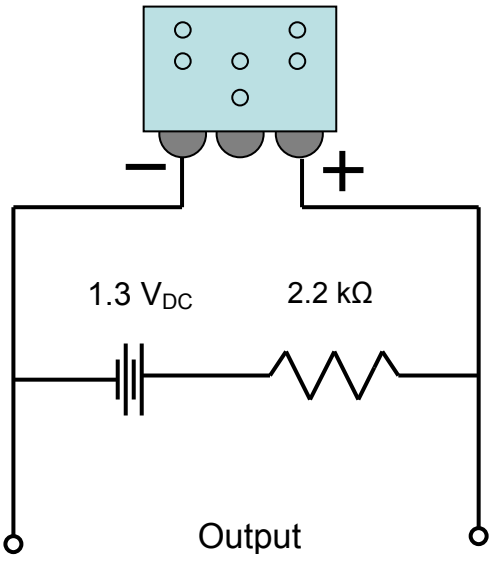

Figure 48. WP-3501 microphone circuit.

To compare the performance of the two microphones, the peak to peak (V_{pp}) voltages from the two microphones (packaged and reference) were compared. Data was taken at frequencies from 300 Hz to 5 kHz for the Knowles WP-3501 microphone using both the stainless steel and all polyurethane packages.

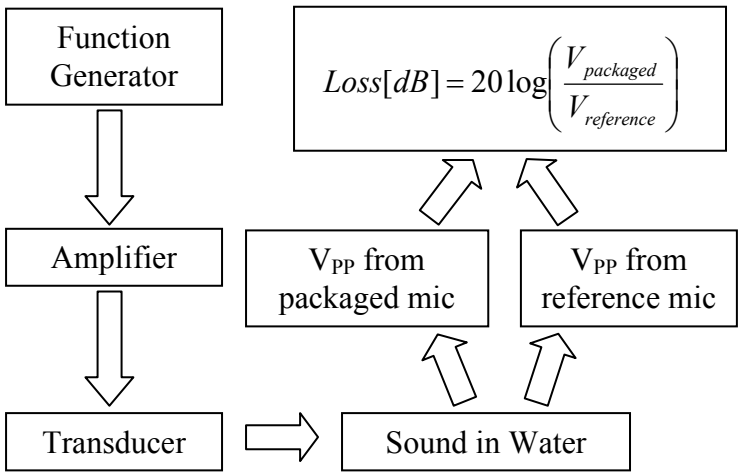

Figure 49. A schematic of the test setup.

The digital oscilloscope was used to measure the peak to peak voltage of the two signals, packaged and reference. Figure 50 shows an example of a typical trace from a test. $V_{pp,\ packaged}$ and $V_{pp,\ reference}$ were measured by the scope at 5.2 mV and 11.mV, respectively. Using equation 4 the loss for that test is calculated to be -6.8 dB.

$$Loss[dB] = 20\log\left(\frac{V_{packaged}}{V_{reference}}\right) \qquad (4)$$

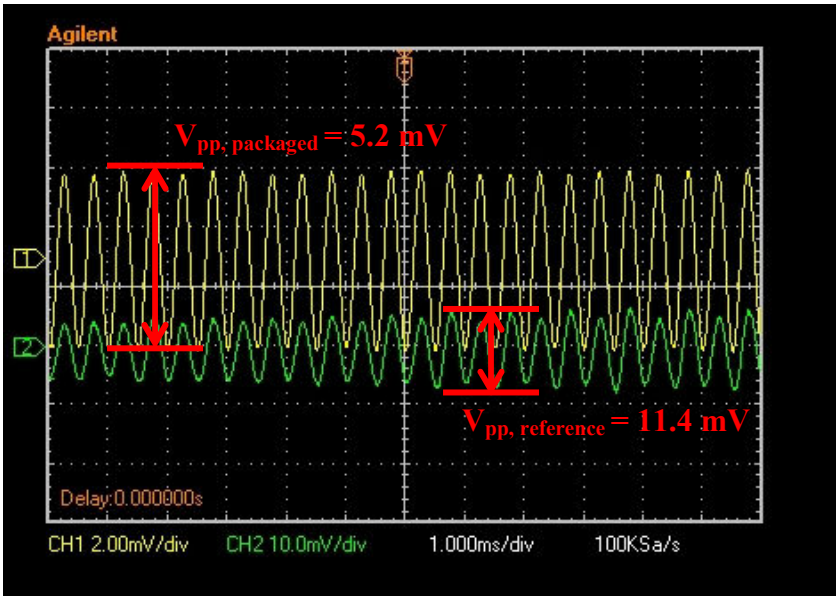

Figure 50. An image from the oscilloscope for a test at 2 kHz on the all polymer package.

The acoustic test package using the stainless steel housing was fabricated and tested first. Results, plotted in Figure 51, show an average loss of -24 dB above a frequency of 2 kHz. Below 2 kHz, the loss increases as frequency decreases. At 300 Hz, the lowest frequency tested, the loss was measured at -51 dB.

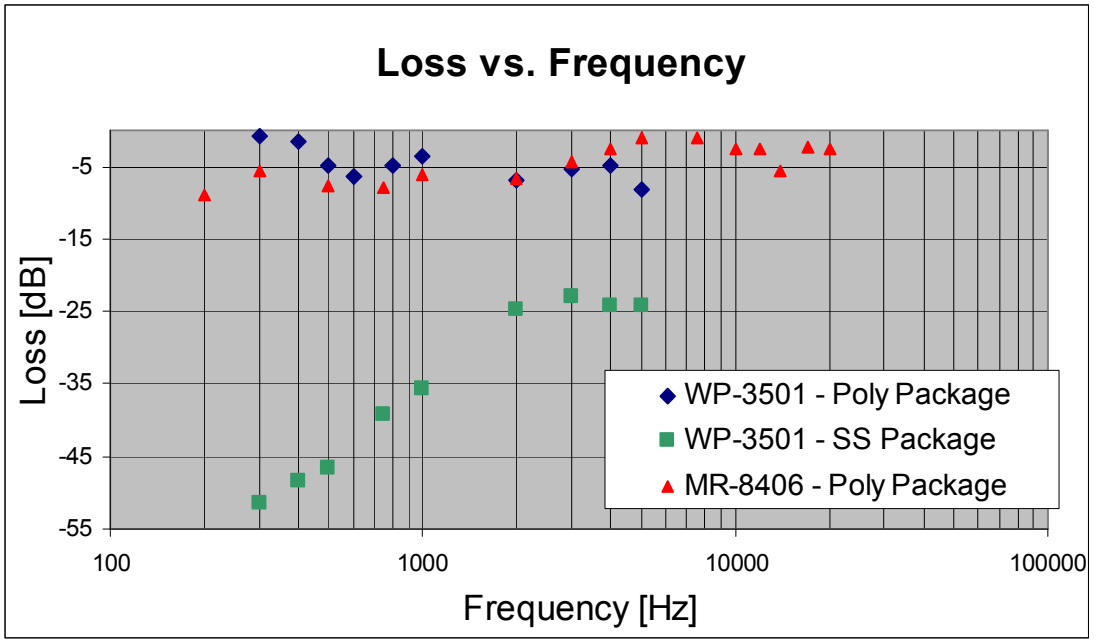

Figure 51. Results from the acoustic testing. Loss vs. frequency.

The high loss, especially at low frequencies, may be due to the interaction of the sound waves with the stainless steel structure. To remove any loss due to the stainless steel structure from the package, the all polymer package was designed and fabricated. Test results are plotted in Figure 51 along with the data from the stainless steel package. Over all loss due to the package over the entire frequency range is improved. Furthermore, the increase of loss at low frequencies is no longer a problem. The average loss for tests done from 300 Hz to 5 kHz is -4.7 dB with a standard deviation of 2.2 dB.

In order to extend the frequency range of the testing, which was limited by the performance of the Knowles WP-3501 microphone, a second round of testing was performed using a new microphone. The Knowles MR-8406 is another waterproof

microphone that worked for frequencies up to 20 kHz. An all-polyurethane package was fabricated to accommodate the larger MR-8406.

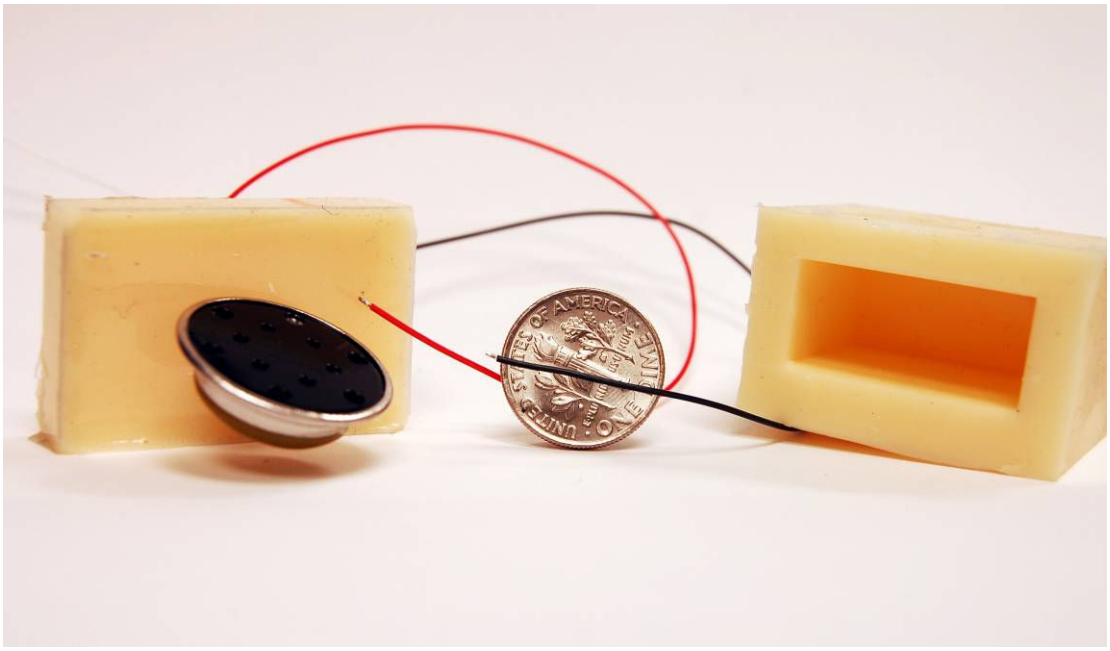

Figure 52. The Knowles MR-8406 and the all-polyurethane package.

The package was tested in the same setup as the WP-3501, with the V_{pp} of an unpackaged microphone used as the reference against a packaged one. Figure 53 shows the circuit built for powering the microphone and monitoring output.

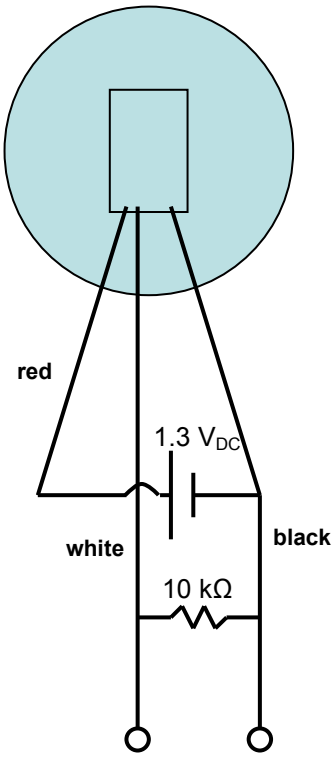

Figure 53. Circuit used for powering and monitoring the MR-8406 microphone.

The new microphone was tested from 200 Hz to 20 kHz. The average loss over the test frequency range was -4.5 dB with a standard deviation of 2.6 dB. The new MR-8406 microphone reinforced the measurements taken by the WP-3501 and extended the testing range to the limits of human hearing.

5.2 Salt Permeation Tests

The rate of salt permeation into the package will directly affect the reliability of the sensor. Not only will salt ions within the fluid medium short out electrical connections (the I/O for the GMR sensors) within the package, but it will aid in the corrosion of the iron-gallium nanowires. The data collected by the test described in this section will be able to be used in the future to determine a predicted lifetime of the sensor and package. Currently there is no data on the corrosion of Galfenol

nanowires and how sensitive they are to the concentration of salt in the water. Investigation into the corrosion of bulk Galfenol has shown that it behaves similarly to carbon steel [23]. Corrosion may be exacerbated at the nanowire scale due to the increase in surface area to volume ratio. With more samples of Galfenol nanowires, such information would be possible to obtain.

5.2.1 Moisture Absorption

There are currently no guidelines or requirements for the minimum moisture absorption of a polyurethane encapsulant [24]; however, it is recommended by Ting that the material not have a weight change greater than 1.4% after 48 hours in seawater at room temperature [25]. Twelve cylindrical samples (Figure 54) were molded of the RenCast 6400 and soaked in a 3.5 wt% salt solution at room temperature for the 48 hours. The weights of the samples were measured with a Mettler AE1000 mass balance. The average weight gain for the twelve samples was 0.85 % with a standard deviation of 0.025 %. By the standard proposed by Ting et al., the RenCast 6400 is a suitable polyurethane encapsulant for use in underwater transducer applications.

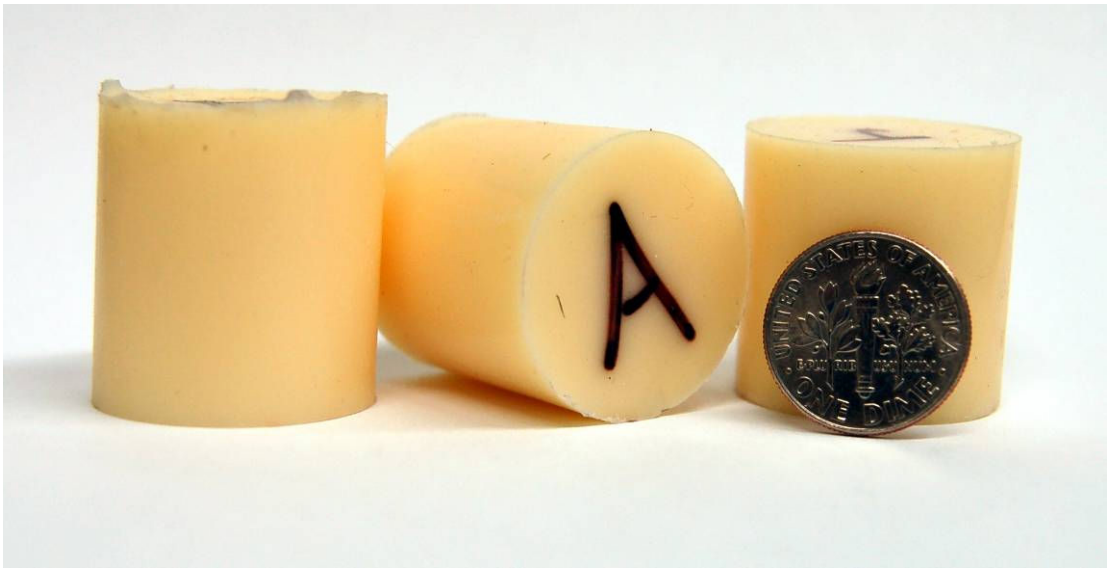

Figure 54. Several of the polyurethane cylinders used for the moisture absorbtion test.

5.2.2 Conductivity Change

Four all polyurethane test packages, identical to the ones used for the acoustic tests of the Knowles WP-3501 microphone, were fabricated. The packages had two bare leads (molded through the lids of the package) inside them instead of microphones. The leads were used for measuring the conductivity of the fluid inside. The packages were filled with DI water and submerged in 3.5 wt% salt solution at room temperature. The conductivity of the DI water was measured every 3 days for 24 days. The resistance across the two leads was monitored with a Fluke multimeter. The multimeter probes were attached to the two wires that were molded into the package. The reading would fluctuate for several minute until settling at a final value, as a result the multimeter was allowed to settle for at least 20 minutes before a reading was taken. Only a slight decrease was measured over the test period, however the change did not constitute a substantial contamination by the salt water. For example, the conductivity for DI water is 0.1 – 10 μS/cm. If the water was

contaminated to the point where it would become comparable to tap water its conductivity would have risen to 100 – 1000 µS/cm., which would be at least a factor of 10. Seawater with a salinity of 35 ppt has a conductivity between 45,000 and 80,000 µS/cm.

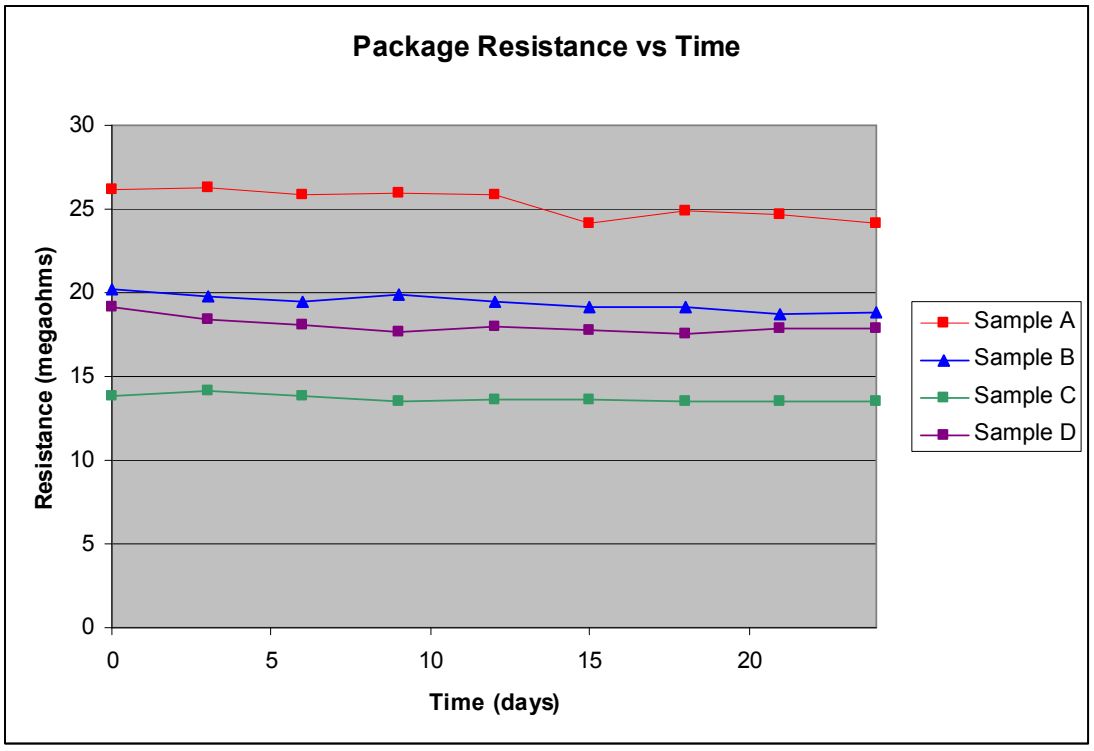

Figure 55. Resistance vs. Time for the four test packages.

Chapter 5: Conclusions

Challenges unique to the design of packaging of a Galfenol nanowire acoustic sensor were identified. Hermetic packages or encapsulation that has been employed in the packaging of other underwater electronics and sensors would not allow sound to reach the nanowires and/or restrict their movement. A bio-inspired prototype package addressing those challenges based on the hearing of fish and other aquatic animals was designed to allow sound to reach the delicate nanowire sensor while protecting it from the harsh underwater environment. The design incorporates impedance matching materials that minimized the reflections caused when sound travels through material interfaces. Material selection was performed using a custom designed setup in a scanning acoustic microscope to measure the acoustic wave speed in candidate materials. Polyurethane rubber for the acoustically transparent window and castor oil for the fluid medium were selected. The materials were incorporated with MEMS fabrication processes to construct a prototype package. The package consists of a micromachined silicon base bonded to a glass lid. Openings were sealed with the polyurethane rubber to allow sound to enter the package. The cavity containing the sensor was filled with castor oil to allow the movement of the nanowires. Testing was performed to investigate the effectiveness of the impedance match between the selected materials. An evaluation of the moisture absorption and salt permeation of the acoustic window material was also done and results presented.

Appendix

Manufacturer's Specifications for the Knowles WP-3501

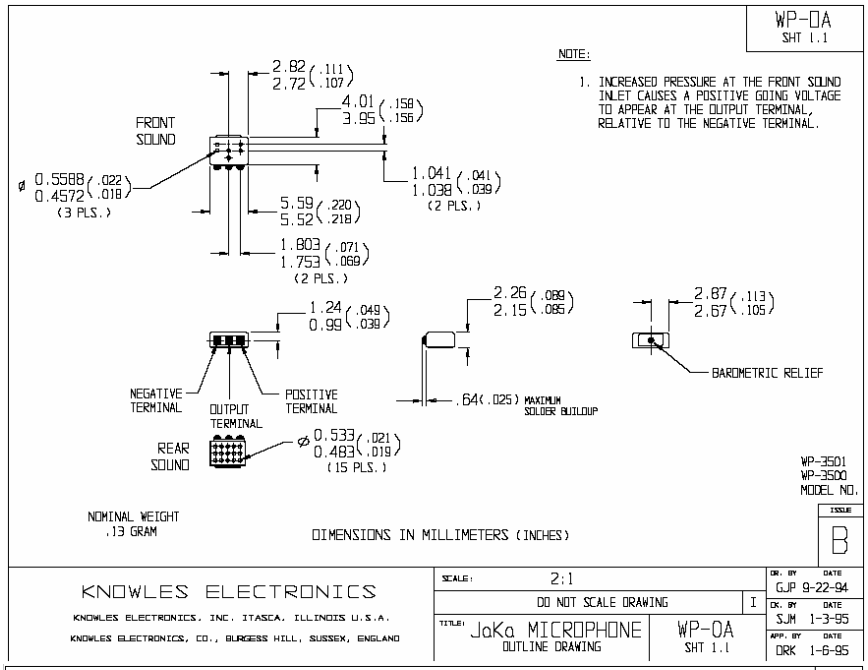

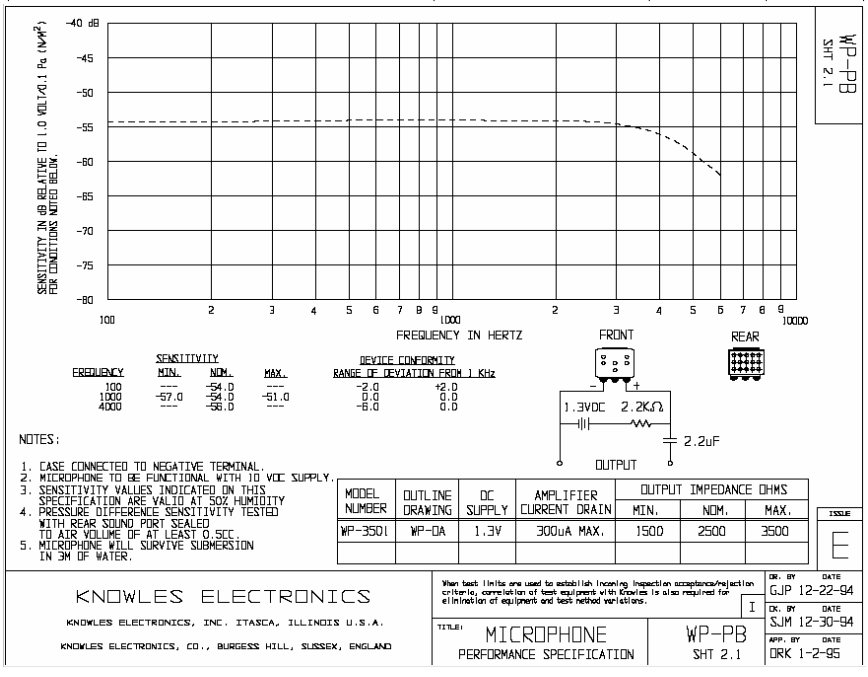

Manufacturer's Specifications for the Knowles MR-8406

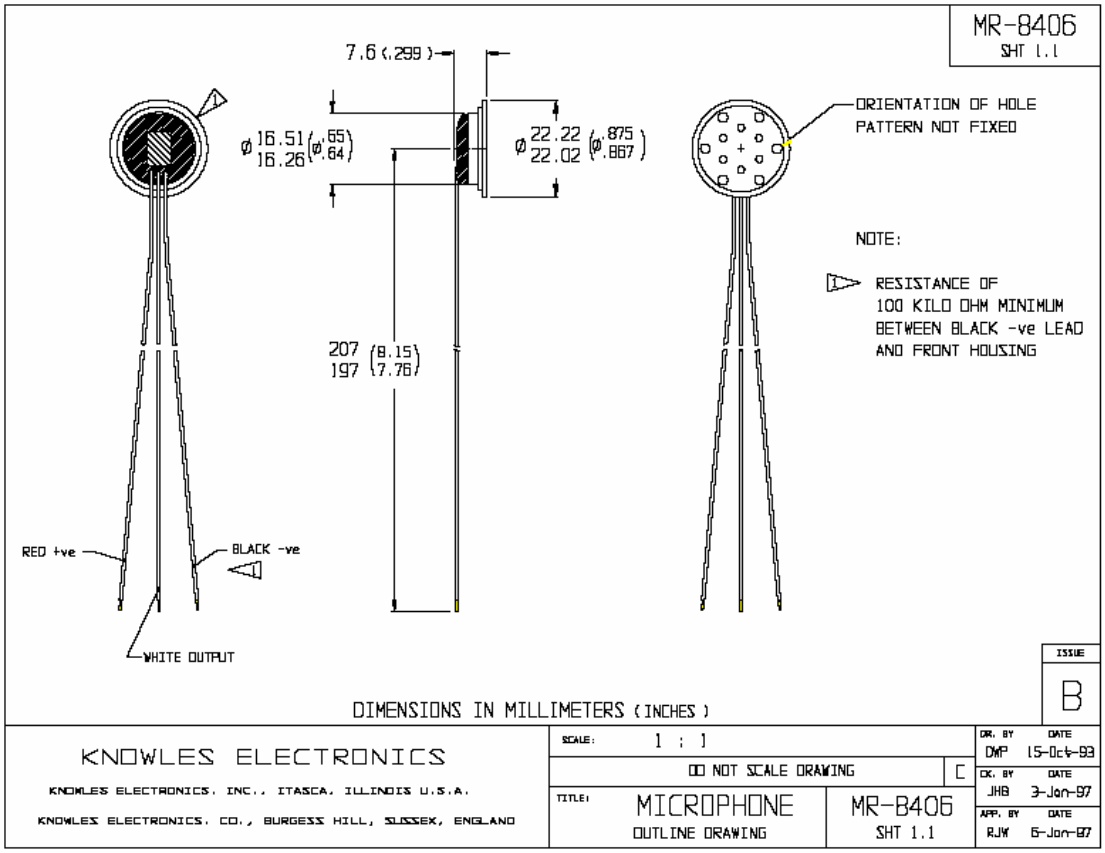

NO DAMPING | MR-8406 SHT 2.1

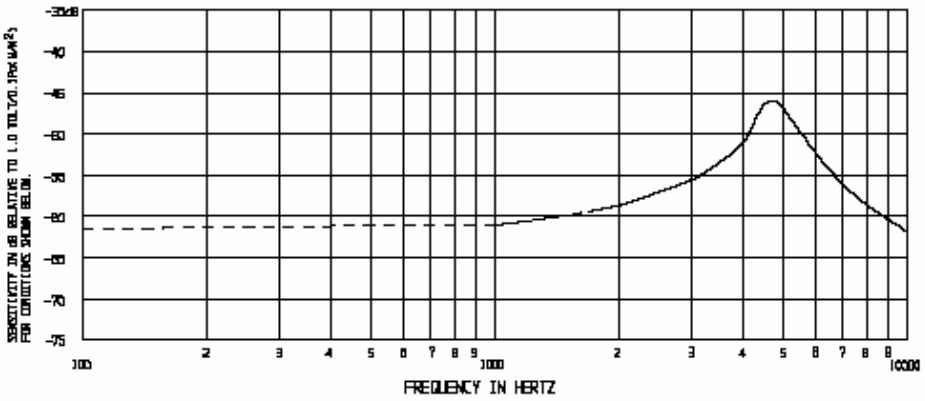

NOTES:

1. CASE OF MICROPHONE CONNECTED TO NEGATIVE BLACK LEAD.
2. BELLOWS HOUSING INSULATED FROM MICROPHONE CASE.
3. MICROPHONE TO BE FUNCTIONAL WITH 20 VDC SUPPLY.
4. CONFORMS TO REQUIREMENTS SHOWN ON "ELECTRET MICROPHONE ENVIRONMENTAL QUALIFICATION TEST, BT-1959 SHEET 2.2

5.

	SENSITIVITY			DEVICE CONFORMITY	
FREQUENCY	MIN.	NOM.	MAX.	RANGE OF DEVIATION FROM 1 KHz	
100	---	-51.5	---	-4.0	+1.0
1000	-55.0	-51.0	-58.0	---	---
4700 APPROX	---	-48.0	---	+8.0	+20.0

6. INDIVIDUAL SPECIFICATIONS.

MODEL NUMBER	OUTLINE DRAWING	LOAD RESISTANCE ON OUTPUT FOR SENSITIVITY MEASUREMENT OHMS	DC SUPPLY V	OUTPUT IMPEDANCE OHMS			AMPLIFIER CURRENT DRAIN µA MAX	SENSITIVITY CHANGE ON REDUCING SUPPLY TO .8VDC	"A" WEIGHTED NOISE (1kHz EQUIVALENT SPL) dB SPL MAX
				MIN.	NOM.	MAX.			
MR-8406	MR-8406	10000	1.3	2000	3500	8000	50	3 dB MAX	30

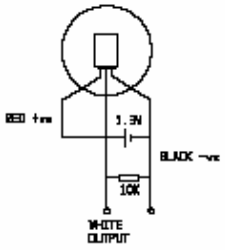

ISSUE A

KNOWLES ELECTRONICS

KNOWLES ELECTRONICS, INC. ITASCA, ILLINOIS U.S.A.

KNOWLES ELECTRONICS, CO., BURGESS HILL, SUSSEX, ENGLAND

Shortest limits are used to establish incoming inspection acceptance/rejection criteria, correlation of test equipment with theories is also required for elimination of equipment and test method variations.

C

TITLE: MICROPHONE PERFORMANCE SPECIFICATION | MR-8406 SHT 2.1

	BY	DATE
ISS.	RW	15-Nov-96
CH.	JHB	3-Jan-97
APP.	RJW	6-Jan-97

References

1. A.E. Clark, J. B. Restorff, M. Wun-Fogle, T. A. Lograsso, D. L. Schalgel, "Magnetostrictive properties of body-centered cubic Fe-Ga and Fe-Ga-Al alloys," IEEE Trans. Magn. 36, 3238-3240, 2000.
2. R. A. Kellogg, Ph.D. thesis, Engineering Mechanics, Iowa State University, Ames, IA, 2003. Available at http://www.aero.umd.edu/~aflatau/TechPubs/Kellogg_2003_Dissertation.pdf
3. P.R. Downey and A.B. Flatau, "Magnetoelastic Bending of Galfenol for Sensor Applications," J. Appl. Phys. 97, (2005).
4. P.D. McGary, L. Tan, J. Zou, B.J.H. Stadler, P.R. Downey, and A.B. Flatau, "Magnetic Nanowires for Acoustic Sensors," J. Appl. Phys. 99, (2006).
5. D.A. Dikin, X. Chen, W. Ding, G. Wagner, and R.S. Ruoff, "Resonance vibration of amorphous SiO_2 nanowires driven by mechanical or electrical field excitation," J. Appl Phys. 93, no. 1, pp. 226-230, (2003).
6. M. Yu, G.J. Wagner, R.S. Ruoff, and M.J. Dyer, "Realization of parametric resonances in a nanowire mechanical system with nanomanipulation inside a scanning electron microscope," Physical Review B, **66**, 073406, (2002)
7. M. Yu, M. J. Dyer, G.D. Skidmore, H.W. Rohrs, X. Lu, K.D. Ausman, J.R. Von Ehr and R.S. Ruoff, "Three-dimensional manipulation of carbon nanotubes under a scanning electron microscope," Nanotechnology, 10, pp. 244-252, 1999.
8. P.R. Downey and A.B. Flatau. "Manipulation and Characterization of Galfenol Nanowires," Poster and presentation at 2006 US Navy Workshop on Acoustic Transduction Materials and Devices, May 9-11, State College, PA, 2006.
9. J.L. Bernstein, S.L. Finberg, K. Houston, L.C. Niles, H.D. Chen, E. Cross, K.K. Li, and K. Udayakumar, "Micromachined high frequency ferroelectric sonar transducers," IEEE Transactions on Ultrasonics, Ferroelectrics, and Frequency Control, vol. 44, no. 5, pp 960-969, 1997.
10. J. Bernstein, "A micromachined condenser hydrophone," Solid State Sensor and Actuator Workshop, 5th Technical Digest, IEEE, pp. 161-165, 1992.
11. S. Alkoy, J. Cochran, and R. Newnham, "Miniature hydrophones from hollow ceramic spheres," Proceedings of the Eleventh IEEE International Symposium on Applications of Ferroelectrics, pp 345-348, 1998.
12. M. Mescher, K. Houston, J. Bernstein, G. Kirlos, J. Cheng, and L.E. Cross, "Novel MEMS microshell transducer arrays for high-resolution underwater acoustic imaging applications," Proceedings of the IEEE Sensors, 1, pp541-546, 2002.
13. B. Zhu and V.K. Varadan, "Integrated MOSFET based hydrophone device for underwater applications," Procedings of SPIE, vol. 4700, pp 101-110, 2002.
14. B. Phillip, J.K. Abraham, V.K. Varadan, and V. Natarajan, "Passive underwater acoustic damping with Rho-C rubber-carbon fiber and molecular sieves," Smart Structures and Materials, **13**, pp. 99-104, 2004.
15. http://www.ai.rug.nl/~tjeerd/CPSP/docs/cochleaModel.html

16. White, R. D. and Grosh, K. "Trapped-Fluid Traveling Wave Filters Based on the Mammalian Cochlea" in Proceedings of the uTAS 2005 Conference, Ninth International Conference on Miniaturized Systems for Chemistry and Life Science, K. F. Jensen, J. Han, D. J. Harrison, and J. Voldman, Eds., pp. 666-668.
17. http://www.glenbrook.k12.il.us/GBSSCI/PHYS/Class/sound/u11l2d.html
18. http://www.life.umd.edu/biology/popperlab/background/orientation.htm
19. Fay, Richard R., and Arthur N. Popper. Comparative Hearing: Fish and Amphibians. New York: Springer, 1999.
20. R.D. Corsaro, J.F. Covey, R.M Young, G Spryn, "Acoustic Coatings for Water-Filled Tanks," Sound and Vibration Damping with Polymers, American Chemical Society, Washington, DC, 1990.
21. CRC Handbook of Chemistry and Physics, Cleveland, Ohio: CRC Press, 2004
22. T. Rude, J. Subramanian, J. Levin, D. Van Heerden, O. Knio, "Hermetic Sealing of Microelectronic Packages Using a Room Temperature Soldering Process," IMAPS Symposium, Philadelphia, Pennsylvania, September 25-29, 2005.
23. L.M. Cheng and Y. Wang, "Corrosion Behaviour of Galfenol in 3.5% NaCl Solution," Presentation at 2006 US Navy workshop on Acoustic Transduction Materials and Devices, State College, PA, May 8, 2006.
24. T. Ramotowski, K. Jenne, "NUWC XP-1 polyurethane-urea: a new, "acoustically transparent" encapsulant for underwater transducers and hydrophones," OCEANS 2003 Proceedings, v. 1, pp. 227-230, 2003.
25. R.Y. Ting, "A new approach to the quality analysis of transducer elastomers," *Elastomerics*, v. 117, no. 8, pp. 29-35, 1985.